The role of HDAC8 in the maintenance of mitotic fidelity

Dissertation

Flávia Machado Santos

Master's degree in Cellular and Molecular Biology

Biology Department

2019/2020

Supervisor

Paula Maria Vieira Jorge, TSS, CHUP

Co-supervisor

Ariana Jácome de Azevedo, Junior Researcher, i3S

STATEMENT OF INTEGRITY

I, Flavia Machado Santos, with up201808610 student number, of the 2018/2019 edition of master's degree in Cellular and Molecular Biology, hereby declare having conducted this academic work with integrity. I confirm that I have not used plagiarism or any form of undue use of information or falsification of results along the process leading to its elaboration. I further declare that I have fully acknowledged the Code of Ethical Conduct of the University of Porto.

Porto, November 11th, 2020

Flávia Machado Santos

ACKNOWLEDGMENTS

Several people had a direct or indirect impact on the culmination of my journey, which, for me, was more than the last year. I have learned so much and to show my most profound appreciation, here are some deserved acknowledgments.

My first thank you goes to the University of Porto, especially to the Faculty of Sciences for accepting me in the Master's program and all the knowledge I acquired there.

A special thank you goes to my supervisor and co-supervisor, Drª Paula Jorge and Drª Ariana Jacome respectively, for always being so available and helpful, for always guiding me and, for all the good advice. Also, a big thank you to Drª Beatriz Porto for the amazing opportunity of working in her laboratory and for sharing her knowledge with me.

As well as a big thank you to Nuno Maia, Claudia Oliveira, and Barbara Rodrigues for being so helpful and patient with all my doubts and for such a supportive friendship, and for creating a wonderful work environment.

To all the other members of the Chromosome instability & Dynamics laboratory at i3S, Cytogenetic laboratory at ICBAS, and Cytogenetic and Molecular Genetics units at CGMJM for all the teachings, patience, and important advice.

I am also very thankful for all my friends, old or new, who have always pushed me to be my best self, for never giving up on me, and for always being there to listen to me. I love and care about you all.

Finally, and most importantly, I would like to thank all my family. Starting with my boyfriend, Diogo, to always be there for me. Your support, understanding, and encouragement make me believe that I can always go further. To my parents and my sisters, for always believing in me and in my dreams and for being proud of me in every step of this process. I love you with all my heart.

With all my heart, a BIG thank you to all of you!

RESUMO

As deacetilases de histonas (HDACs) representam uma ampla família de enzimas envolvidas num conjunto de mecanismos epigenéticos de regulação génica, via deacetilação, tais como a repressão da transcrição e a condensação da cromatina. Estas enzimas removem os grupos acetil presentes nas lisinas de histonas e não histonas, localizadas quer no núcleo quer no citoplasma. Atualmente estão descritas dezoito HDACs, divididas em quatro classes, sendo que estas têm sido associadas a várias doenças humanas como o cancro e patologias neurodegenerativas. O objetivo deste trabalho é identificar e explorar as funções da proteína HDAC8, uma deacetilase de histonas pertencente à classe I, responsável pela deacetilação de diversas histonas e não histonas. Ao longo dos últimos anos têm sido descritos vários substratos não histonas da HDAC8, contudo o papel fundamental desta proteína em muitos mecanismos celulares vitais mostra que existem substratos ainda por identificar. Um dos substratos da HDAC8 melhor caraterizado é a proteína SMC3, uma subunidade do complexo da coesina que medeia a correta segregação das cromatídes irmãs para polos opostos na mitose e/ou meiose. A perda de atividade da HDAC8 resulta numa acumulação da proteína SMC3 acetilada, levando a uma diminuição da coesina necessária para os próximos ciclos de divisão celular. A falha deste mecanismo devido a um defeito na HDAC8, em humanos, causa uma doença severa e rara, multissistémica com hereditariedade dominante ligada ao X, conhecida como Síndrome de Cornelia de Lange do tipo 5 (CdLS-5). Esta proteína tem sido associada a genes e proteínas envolvidas no cancro como *P53*, p73, SOCS1/3, proteína de fusão inv(16) e proteína telomerase. Adicionalmente, a desregulação da HDAC8 tem sido implicada na proliferação, invasão e apoptose em diferentes tipos de cancro. O mecanismo pelo qual modificações pós-traducionais influenciam a fidelidade mitótica permanece mal compreendido. Atualmente, sabe-se que defeitos no mecanismo mitótico comprometem a sua fidelidade, o que consequentemente poderá resultar em aneuploidias. Estas são uma das maiores causas de anomalias congénitas e um marco da tumorogenese. Recentemente, foi demonstrado, que em oócitos de ratinho esta proteína se localiza nos polos do fuso mitótico e que a sua depleção resulta em erros durante a divisão celular. O deficiente mecanismo mitótico, resulta no desalinhamento dos cromossomas, gerando aneuploidia. Os autores sugerem que a expressão da Hdac8 é assim crucial para a correta formação do fuso mitótico e alinhamento dos cromossomas durante a mitose em estádios precoces da oogénese, permitindo uma normal fertilidade nos ratinhos. O papel da HDAC8 na fidelidade mitótica em células humanas até hoje não foi

reportado. Os objetivos deste estudo são: i) identificar e descrever a localização da HDAC8 nas diferentes fases do ciclo celular; ii) investigar a função da HDAC8 na fidelidade mitótica recorrendo a siRNAs e ii) analisar o impacto de uma variante do gene *HDAC8* na instabilidade cromossómica, em células humanas. Durante a divisão celular, esta proteína foi localizada no fuso mitótico e no *midbody*, co-localizando com a alfa tubulina tirosinada, uma proteína constituinte dos microtúbulos. Estudos de depleção da HDAC8, em células HeLa, revelaram um elevado número de erros mitóticos como, falha na congregação dos cromossomas, cromossomas em atraso (*lagging*), pontes de cromatíde e fusos multipolares, podendo estes defeitos originar aneuploidias. Para uma melhor compreensão das implicações da HDAC8 na manutenção do nível de ploidia recorremos a linhas celulares provenientes de um caso clínico (não publicado) com uma variante no gene *HDAC8* presente em heterozigotia. Esta variante missense, c.793C>T; p.(Gly265Arg), está descrita como patogénica nas bases de dados ClinVar e dbSNP, mas sem informação da sua frequência, podendo assim ser classificada como causal. A análise do nível de ploidia em fibroblastos e linhas linfoblastóides deste caso clínico mostrou a existência de células aneuploides em conformidade com os resultados obtidos das células HeLa. Este estudo sugere assim novas funções da HDAC8 no controlo da instabilidade cromossómica e/ou divisão celular assimétrica, originando aneuploidias que podem ter implicações na predisposição para cancro e/ou defeitos congénitos. O presente estudo trata-se da primeira abordagem conhecida à análise do impacto da HDAC8 na fidelidade mitótica em linhas celulares derivadas de células humanas.

Palavras-chave: HDAC8; gene *HDAC8*; Mitose; Fidelidade Mitótica; Aneuploidia; Instabilidade cromossómica.

ABSTRACT

Histone deacetylases (HDACs) are a large family of enzymes involved in a wide range of epigenetic gene regulation mechanisms such as transcriptional repression and chromatin condensation via deacetylation, removing the acetyl groups of lysines from histone and non-histone proteins located in the cytoplasm and nucleus. Eighteen HDACs, subdivided into four classes have been described so far. Recently, HDACs have been implicated in many human diseases such as cancer and neurodegenerative disorders. This project aims to unravel and comprehend the role of HDAC8 protein, a class I histone deacetylase responsible for the deacetylation of many histone and non-histone substrates. Over the last few years, many HDAC8 non-histone substrates have been identified. Nevertheless, it is widely believed that there are much more substrates to discover, as demonstrated by the crucial role of HDAC8 in many important cellular mechanisms. One of the well-known HDAC8 non-histone substrates is the structural maintenance of chromosomes protein 3 (SMC3). The SMC3 is a subunit of the cohesin complex which mediates the correct segregation of sister chromatids to the opposite poles during mitosis or meiosis. Loss of HDAC8 activity leads to the accumulation of acetylated SMC3, which results in decreased cohesin at localized sites. Consequently, in humans, the impairment of this mechanism, due to an HDAC8 defect, results in Cornelia de Lange Syndrome type 5 (CdLS-5), a very severe and rare X-linked dominant multisystemic disorder. Additionally, HDAC8 has been associated with some genes and proteins involved in cancer, such as *P53*, p73, SOCS1/3, inv (16) fusion protein, and telomerase protein. The deregulation of HDAC8 has been implicated in different types of cancer impairing proliferation, invasiveness, and apoptosis. It is known that defects in the mitotic apparatus assembly compromise mitotic fidelity and consequently lead to aneuploidy. These defects are a major cause of birth anomalies and a hallmark of tumorigenesis. Recently, it was described that mutations in Hdac8 accrue errors during cell division in mouse oocytes, including deficient spindle assembly and chromosome misalignment leading to aneuploidies. The same study revealed that Hdac8 localizes at spindle poles, to participate in chromosome alignment and thus allowing accurate spindle assembly and ensuring ploidy in mouse eggs. The authors suggested that the expression of Hdac8 is required in early oogenesis for correct chromosomal assembly during meiosis and optimal fertility in mice. Herein, we questioned the role of HDAC8 in the chromosomal assembly in human's cells, a process not yet reported. This study aims to i) describe the HDAC8 location on different stages of the cell cycle, ii) investigate the HDAC8 function in mitotic fidelity using siRNAs and iii) analyze the impact of a mutant

HDAC8 allele in chromosome instability. We have found that HDAC8 localizes at the mitotic spindle and the midbody, co-localizing with tyrosinated alpha tubulin, a constituent of microtubules. Furthermore, HDAC8 depletion studies in HeLa cells indicated several mitotic abnormalities, including chromosome congression failure, lagging chromosomes, chromatin bridges and multipolar spindle, all of which can result in aneuploidy. To further understand the implications of HDAC8 in the maintenance of ploidy we used primary cells from a female affected individual presenting a heterozygous *HDAC8* variant. The missense variant c.793C>T; p.(Gly265Arg) is described as likely pathogenic at ClinVar and dbSNP databases, but without frequency information, suggesting a plausible candidate causative variant. Concomitant to the findings in HeLa cells, fibroblasts and LCLs from the same patient shown a significantly high ratio of aneuploid cells revealing new insights into this unique and undescribed affected individual. Overall, the results from this study highlight new functions of HDAC8 in the control of chromosomal instability and/or asymmetric cell division which can lead to aneuploidy and consequently can have implications in predisposition to cancer and/or congenital defects. To the best of our knowledge, this is the first report of HDAC8 impact on mitotic fidelity in human-derived cell lines.

Keywords: HDAC8; *HDAC8* gene; Mitosis; Mitotic fidelity; Aneuploidy; Chromosome instability.

TABLE OF CONTENTS

LIST OF TABLES

LIST OF FIGURES

LIST OF ABBREVIATIONS

%- Percentage

ºC- Degree Celsius

µg- Microgram

µL- Microliter

bp- Basepairs

Kb- Kilobase

kDa- Kilodalton

mL- Milliliter

ng- Nanogram

nM- Nanomolar

nm- nanometer

α-SMA- Alpha Smooth Muscle Actin

α- Alpha

γ- Gamma

β- Beta

A- Adenine

Ac- Acetyl

Ala- Alanine

ALL- Acute Lymphocytic Leukemia

AML- Acute Myeloid Leukemia

Arg- Arginine

ARID1A- AT-Rich Interactive Domain-containing protein 1A

Asn- Asparagine

Asp- Aspartic acid

ATL- Adult T-cell Leukemia

BMF- Bcl2 Modifying Factor

C- Cytosine

CdLS- Cornelia De Lange Syndrome

cDNA- Complementary Deoxyribonucleic Acid

CGM- Centro de Genética Médica Doutor Jacinto Magalhães

CO_2- Carbon Dioxide

CREST- Calcinosis, Raynaud's phenomenon, Esophageal dysmotility, Sclerodactyly and Telangiectasia

Cys- Cysteine

DEB- 1,3-Butadiene diepoxide

DMEM- Dulbecco's Modified Eagle's Medium

DNA- Deoxyribonucleic Acid

ECL- Enhanced Chemiluminescence

EDTA-Ethylenediaminetetraacetic Acid

ERRα- Estrogen-Related Receptor alpha

ESCO- Establishment of Sister Chromatid Cohesion N-Acetyltransferase

F- Forward

FBS- Fetal bovine serum

G- Guanine

g- G-Force

Gln- Glutamine

Glu- Glutamic acid

Gly- Glycine

HCC- Hepatocellular carcinoma

Hda1- Yeast Histone Deacetylase 1

HDAC- Human Histone Deacetylase

His- Histidine

Hos3- Histone deacetylase One Similar 3

HUMARA- Human androgen receptor methylation assay

ICBAS- Instituto de Ciências Biomédicas Abel Salazar

INV- Inversion

i3S- Instituto de Investigação e Inovação em Saúde

Kcl- Potassium chloride

KT-MTs- Kinetochore-microtubules

LCLs- Human-derived lymphoblastoid cell lines

Leu- Leucine

Lys- Lysine

M- Molar

MAPK- Mitogen-activated protein kinase

MAPs- Microtubule-associated proteins

Met- Methionine

MT- Microtubule

MTOC- Microtubule-organizing center

NAD- Nicotinamide Adenine Dinucleotide

NCBI- National Center for Biotechnology Information

NCOA3- Nuclear receptor co-activator 3

NIPBL- Nipped-B-Like

OMIM- Online Mendelian Inheritance in Man

P73- Tumor suppressor protein 73

PCR- Polymerase Chain Reaction

Pro- Proline

R- Reverse

RAD21- Double-strand-break repair protein rad21 homolog

RAI1- Retinoic Acid Induced 1

RCF-Relative Centrifugal Field

RNA- Ribonucleic acid

Rpd3- Reduced Potassium Dependency 3

RPMI- Roswell Park Memorial Institute

RT- Room temperature

RT-PCR- Reverse transcription polymerase chain reaction

Ser- Serine

Sir2- Silent Information Regulator 2

siRNA- Silencing ribonucleic acid

SIRT- Sirtuin

SMAD- Small Mother against Decapentaplegic

SMC1A- Structural Maintenance of Chromosomes 1A

SMC3- Structural Maintenance of Chromosomes 3

SOCS1/3- Suppressor of cytokine signaling 1/3

STAT3- Signal transducer and activator of transcription 3

T- Thymine

Ter- Termination

TGF-β- Transforming Growth Factor Beta

Thr- Threonine

THRAP3- Thyroid Hormone Receptor-Associated Protein 3

P53- Tumor protein 53

Trp- Tryptophan

Tyr- Tyrosine

Val- Valine

WB- Western blotting

WT- Wild-type

XCI- X chromosome inactivation

XIST- X Inactive Specific Transcript

Zn^{+}- Zinc ion

INTRODUCTION

1. Histone deacetylases

Histone deacetylases (HDACs) are known as a large family of enzymes. These enzymes are involved in a wide range of epigenetic gene regulation mechanisms such as transcriptional repression and chromatin condensation, by removing the acetyl groups from amino acid residues (lysines) of histone and non-histone proteins localized in cytoplasm and nucleus, a process known as “deacetylation” (Amin, Adhikari, and Jha, 2017).

HDACs are divided into four main classes based on their phylogeny and sequence homology to yeast orthologues. Classes I, II, and IV include the “classical” metal-dependent HDAC enzymes, responsible for the regulation of thousands of proteins, and characterized by the presence of a zinc catalytic binding domain (Zn^{2+}-dependent) (Table 1). Class III consists of the Sirtuins (SIRT 1 to 7) which share homology with the yeast silent information regulator 2 (Sir2). Sirtuins are called nonmetal-dependent enzymes due to the consumption of nicotinamide adenine dinucleotide to deacetylate the lysine residues (NAD^+-dependent) (Table 1) (Gregoretti, Lee, and Goodson, 2004; Haberland, Montgomery, and Olson, 2009; De Ruijter et al., 2003; Witt et al., 2009). In sum, they can also be divided into two main groups belonging to the classical HDACs family (class I, II, and IV) which require zinc (Zn) ions or on the other hand, class III (Sirtuins) depend on NAD+ as cofactors.

In 1996, Schreiber and coworkers described, for the first time, a mammalian HDAC catalytic subunit, HD1 or HDAC1, very similar to the yeast transcriptional regulator, Rpd3 (Taunton, Hassig, and Schreiber, 1996). Subsequently, seventeen HDACs proteins have been identified (Table 1) (Dokmanovic, Clarke, and Marks, 2007).

Table 1 Information about eighteen histone deacetylases from the human. (Adapted from UniProt and The Human Protein Atlas)

Class	Yeast HDAC	Human HDAC	Dependent on	Distribution	Subcellular location
Class I	Rpd3	HDAC1 (UniProt #Q13547)	Zn^{2+}	Low tissue specificity	Nucleus
		HDAC2 (UniProt #Q92769)	Zn^{2+}	Low tissue specificity	Nucleus and cytoplasm
		HDAC3 (UniProt #O15379)	Zn^{2+}	Low tissue specificity	Nucleus, cytoplasm, and cytosol
		HDAC8 (UniProt #Q9BY41)	Zn^{2+}	Low tissue specificity	Nucleus and cytoplasm
Class II	Hda1	HDAC4 (UniProt #P56524)	Zn^{2+}	Tissue enhanced (skeletal muscle)	Nucleus and cytoplasm
		HDAC5 (UniProt #Q9UQL6)	Zn^{2+}	Low tissue specificity	Nucleus and cytoplasm
		HDAC7 (UniProt #Q8WUI4)	Zn^{2+}	Tissue enhanced (lymphoid tissue)	Nucleus and cytoplasm
		HDAC9 (UniProt #Q9UKV0)	Zn^{2+}	Low tissue specificity	Nucleus
		HDAC6 (UniProt #Q9UBN7)	Zn^{2+}	Low tissue specificity	Nucleus, cytoplasm, cytoskeleton, dendrite, axon
		HDAC10 (UniProt #Q969S8)	Zn^{2+}	Low tissue specificity	Nucleus, cytoplasm
Class IV	Hos3	HDAC11 (UniProt #Q96DB2)	Zn^{2+}	Low tissue specificity	Nucleus
Class III	Sir2	Sirtuin-1 (UniProt #Q96EB6)	NAD^+	Low tissue specificity	Nucleoplasm, cytoplasm, and mitochondria.
		Sirtuin-2 (UniProt #Q8IXJ6)	NAD^+	Tissue enhanced (brain, skeletal muscle)	Plasm membrane, cytoskeleton, nucleus, cytoplasm, chromosome, and midbody
		Sirtuin-3 (UniProt #Q9NTG7)	NAD^+	Low tissue specificity	Mitochondrion
		Sirtuin-4 (UniProt #Q9Y6E7)	NAD^+	Low tissue specificity	Mitochondrion
		Sirtuin-5 (UniProt #Q9NXA8)	NAD^+	Low tissue specificity	Mitochondrion, cytosol, and nucleus
		Sirtuin-6 (UniProt #Q8N6T7)	NAD^+	Low tissue specificity	Nucleus
		Sirtuin-7 (UniProt #Q9NRC8)	NAD^+	Low tissue specificity	Nucleolus, nucleoplasm, chromosome, and cytoplasm

Class I contains HDAC1, HDAC2, HDAC3, and HDAC8 proteins that are localized mainly in the nucleus and/or cytoplasm with low tissue specific expression, sharing homology with yeast Rpd3 (Table 1) (Dokmanovic, Clarke, and Marks, 2007).

Class II is characterized by sharing homology with yeast Hda1, and is subdivided in IIa: HDAC4, HDAC5, HDAC7, and HDAC9, and IIb consisting of HDAC6 and HDAC10. Class IIa HDAC4 and 7 show a tissue-specific distribution, skeletal muscle and lymphoid tissue respectively, whereas HDAC5 and 9 show low tissue specificity. These HDACs

are localized between the nucleus and/or cytoplasm. Class IIb is localized mainly in the nucleus and cytoplasm with low tissue specific distribution (Table 1).

Class IV is composed of the HDAC11 deacetylase, which shares homology with yeast Hos3, which is distributed in a low tissue-specific manner with a nucleus location. HDAC11 catalytic center has several conserved residues common among class I and class II deacetylases (Kutil et al., 2018). Class III of the deacetylases consists of Sirtuins (SIRT1-7) and that were characterized based on their homology with yeast Sir2. Those are structurally and mechanistically distinct from other HDACs (Seto and Yoshida, 2014), with low tissue specific distribution with exception of SIRT2, with tissue enhanced in the brain and skeletal muscle. Sirtuins show a wide subcellular location such as nucleus, cytoplasm, mitochondrion and chromosomes (Table 1).

The function of all classes of HDACs was traditionally attributed to nuclear enzymes involved in the deacetylation of histone substrates known to regulate gene expression altering chromatin architecture. However, in the last years, improvements in proteomics, computational and modeling analyses allowed the identification of many non-histone proteins as primary substrates of some HDACs such as the case of HDAC8 (Gregoretti, Lee, and Goodson, 2004). Examples of non-histone proteins include transcription factors, DNA-repair enzymes, chaperones, signal-transduction molecules, and DNA-binding proteins (Ververis et al., 2013). Many biological processes such as differentiation, proliferation, apoptosis, and senescence (De Ruijter et al., 2003; Waltregny et al., 2004) are described to be altered depending on the HDACs proficiency. Therefore, HDACs are involved in the occurrence and progression of a number of pathophysiological conditions and diseases such as inflammation, autoimmune diseases, metabolic dysfunctions, neurodegenerative disorders and cancer. HDAC enzymes have become an interesting and crucial target to fight disease, especially cancer (Nian et al., 2009). The abnormal deacetylation activity and expression became a very popular and interesting topic to understand cancer generation and progression (Budillon et al., 2007; Chakrabarti et al., 2015; Gallinari et al., 2007; Vanaja, Ramulu, and Kalle, 2018). Studying the involvement of those genes and its products in genomic instability is of crucial interest, to increase understanding of cancer pathways.

1.1. HDAC8, a class I histone deacetylase

1.1.1. Characterization of *HDAC8* gene

In 2000, Clarck J. and coworkers cloned and characterized the complete nucleotide sequence of *HDAC8* cDNA. *HDAC8* (NCBI GeneID:55869) gene encodes the human histone deacetylase 8 protein, HDAC8 (Buggy et al., 2000). Wyngaert I. et al. reported the *HDAC8* cDNA shows high similarity to *HDAC1* (54%), *HDAC2* (54%) and *HDAC3* (39%) cDNA sequences, making that a class I histone deacetylase enzyme. Like *HDAC6*, *HDAC8* is an X-linked gene, located at q13.1 position (Figure 1A) and comprising 11 exons with a reading frame sequence of 1754 bp (Figure 1B) (Wyngaert et al., 2000; Ensembl: ENST00000373573.9).

Interestingly, *HDAC8* location is near to the breakpoints associated with preleukemia, in Xq13 (Wyngaert et al., 2000), and to X Inactive Specific Transcript *(XIST)*, in Xq13.2 (Figure 1B), a gene that encodes a non-coding RNA, Xist, which is the main effector of X-chromosome inactivation (XCI) in females (OMIM #314670). The process of XCI is an epigenetic mechanism of dosage compensation, where one of the X chromosomes in females is randomly silenced by modification of chromatin composition and structure in the early stages of embryogenesis (Fang, Disteche, and Berletch, 2019).

Usually when a female carries a “severe” mutant allele at the X chromosome a complete skewing of the X inactivation pattern occurs, so that the mutated X chromosome is not expressed. It is also possible that the skewing is not complete in many tissues and the female expresses the mutant allele as in the case of *HDAC8* pathogenic variants implicated in Cornelia de Lange syndrome type 5 (CdLS-5).

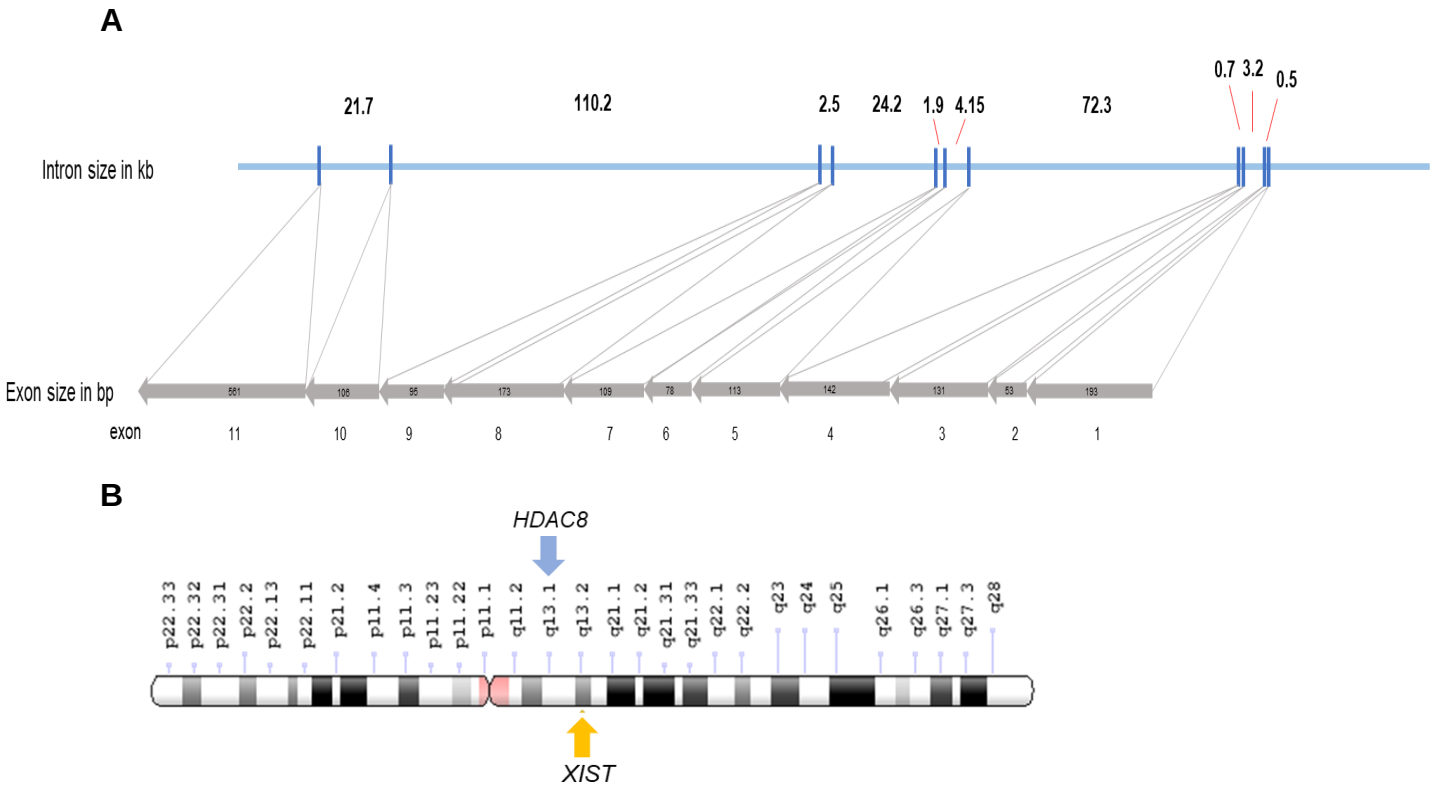

Figure 1 Human *HDAC8*gene.

A) Human *HDAC8* gene structure (not at scale): *HDAC8* gene comprises 11 exons with a coding sequence length of 1754 bp. In the upper image, exons are represented at dark blue, and the introns at light blue. Introns sizes are indicated (kb). In the lower image, exons are represented by grey arrows, which indicate gene orientation, numbered below. Exon sizes are also indicated within the arrows (bp) (Adapted from Ensembl database).
B) *HDAC8* location in X chromosome. *HDAC8* localize in X chromosome at q13.1 position, near to the *XIST* gene (Xq13.2) (Adapted from Ensembl database).

1.1.2. HDAC8 protein structure and its substrates

1.1.2.1. HDAC8 structure

HDAC8 protein is composed of 377 amino acids, with a predicted molecular mass of approximately 42kDa (UniProt #Q9BY41-1), being the smallest isoform among the HDACs present in class I and the second shortest of HDACs family, just after HDAC11. Unlike other HDACs, Human HDAC8 is an X-linked protein which it is not dependent on any co-complex for the activity (Buggy et al., 2000; Chakrabarti et al., 2015; Hu et al., 2000; Wyngaert et al., 2000).

Structurally HDAC8 consists of a nuclear location sequence present between the catalytic domain of the enzyme and a serine binding motif at the end of the HDAC catalytic domain (Banerjee et al., 2019) (Figure 2). Recently, the functional and structural

importance of the conserved glycine-rich loop G302GGGY in the active site of HDAC8 was identified. Missense and nonsense mutations in this HDAC8 loop were described as the underlying cause of CdLS-5 (Liu and Krantz, 2009; Porter et al., 2016).

HDAC8 has been extensively studied as being the best kinetically and structurally characterized HDAC. However, a vast amount of information has yet to be determined regarding the cohort of HDAC8 substrates and binding partners, cellular location, and regulatory mechanisms. The dissection of these factors will be crucial for understanding the detailed function of HDAC8.

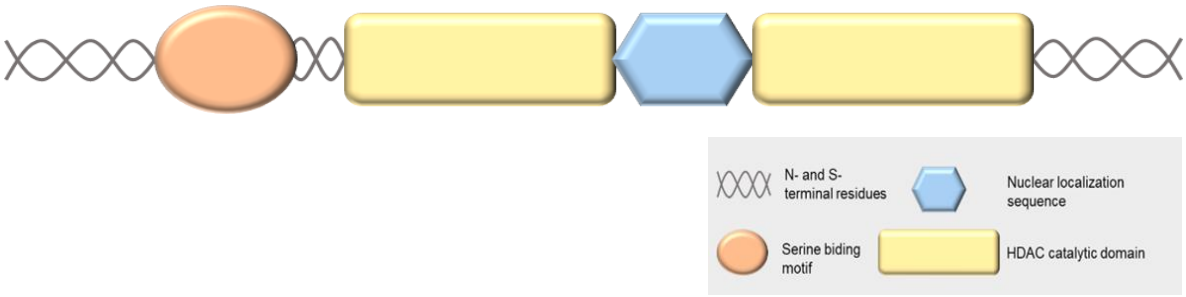

Figure 2 Schematic representation of Histone deacetylase 8 domains (Adapted from Amin, Adhikari, and Jha, 2017).

1.1.2.2. HDAC8 substrates

HDAC8 was initially described to be involved in the deacetylation of histone substrates leading to global chromatin condensation and transcription repression (Seto and Yoshida, 2014). First reports identified HDAC8 as the deacetylase of histones full-length H2A/H2B, H3 and H4 at nonspecific acetylated lysines (Figure 3) (Buggy et al., 2000; Wolfson, Pitcairn, and Fierke, 2013; Wyngaert et al., 2000). In subsequent years some histone-tail derived peptides were reported as HDAC8 substrates; among those are H4 histone tail acetylated lysines (Kac) 14, 16, and 20, and H3 histone tail acetylated lysines (Kac) 14 and 16 (Figure 3) (Buggy et al., 2000; Dose et al., 2011; Hu et al., 2000). However, the histone substrates of HDAC8 remain controversial *in vivo*. On the other hand, non-histone substrates were also described for HDAC8. Importantly, many different biological processes, such as sister chromatid separation, energy homeostasis, microtubule integrity, and muscle contraction have been reported as a consequence of non-histone substrates deacetylated by HDAC8 (Deardorff, Bando, et al., 2012; Li et al., 2014; Wilson et al., 2010).

In the last years, different non-histone substrates were identified such as p53 (Wu et al., 2013) and the Acute Myeloid Leukemia (AML) associated protein inv(16) fusion protein (Figure 3) (Durst et al., 2003). Also, retinoic acid-induced 1 (RAI1), zinc finger, RAN-binding domain containing 2 (ZRANB2), nuclear receptor co-activator 3 (NCOA3) and thyroid hormone receptor-associated protein 3 (THRAP3) have been reported as non-histone substrates (Oslon et al., 2014). Other HDAC8 non-histone substrates were identified only *in vivo* such as structural maintenance of chromosomes 3 (SMC3) (Deardorff, Bando et al., 2012), ERRα (Wilson et al., 2010), cortactin (Li et al., 2014) and ARID1A (Oslon et al., 2014) (Figure 3). Other proteins such as α-actin (Waltregny et al., 2005), CREB (Gao et al., 2009), Hsp20 (Karolczak-Bayatti et al., 2011), DEC1 (Qian et al., 2014) high mobility group protein B1, peroxiredoxin 6, phosphoglycerate mutase 1 and Parkinson protein 7 (Lopez et al., 2015) have been found to be related with HDAC8, yet it is unclear whether these proteins form a part of complex in which HDAC8 acts as a scaffold or are direct acetylation targets. Nevertheless, a wide range of substrates was identified in peptide arrays associated directly or indirectly with HDAC8 indicating further physiological substrates to be discovered (Alam et al., 2016).

In summary, contrary to initial findings, HDAC8 protein involvement it is not limited to the deacetylation of substrates involved in gene expression (histone substrates) but also a wide range of other products (non-histone) implicated in different cellular processes such as senescence, proliferation, differentiation and even tumorigenesis. The understanding and identification of those substrates revealed to be crucial in the development of new therapeutic strategies and targets for a wide and different range of human diseases.

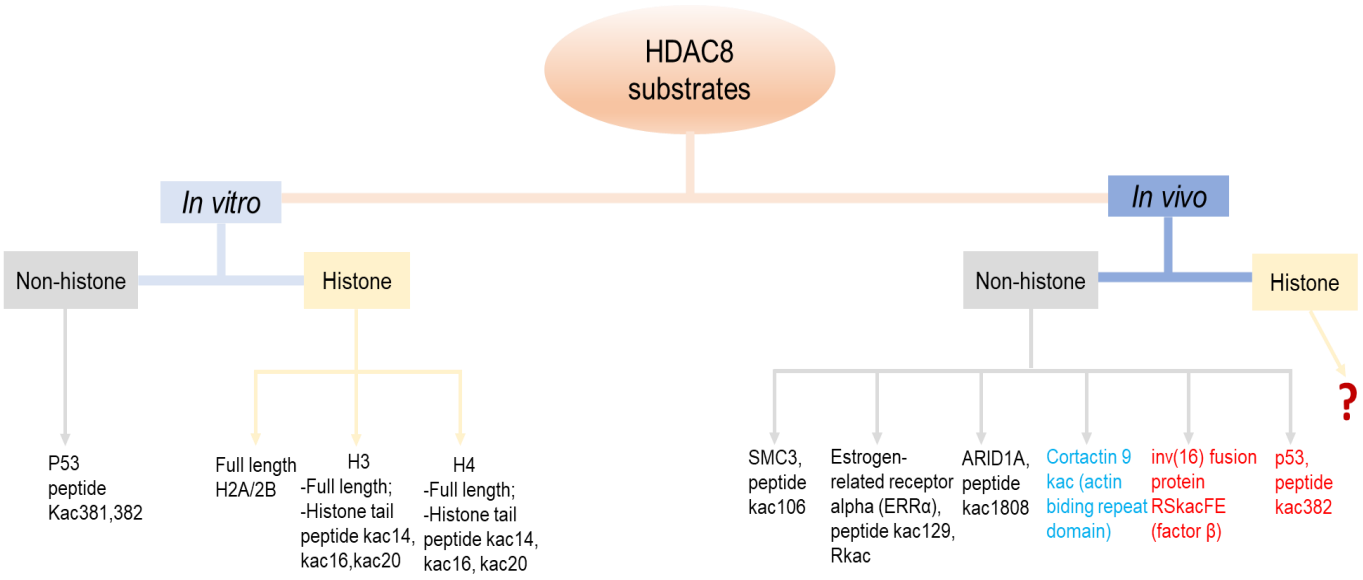

Figure 3 Identification of Histone deacetylase 8 deacetylation substrates.

In vitro, HDAC8 deacetylates both histone and non-histone substrates. *In vivo*, HDAC8 histone substrates remain controversial, while non-histone substrates seem to be the major deacetylation substrates. Representative location, nuclear and cytoplasmic, of non-histone substrates are shown, nuclear location in black, cytoplasmatic location in blue, and nuclear and cytoplasmatic location in red. RKac and RSKacFE represent specific motifs that associate with HDAC8 (Adapted from Chakrabarti et al., 2015)

1.1.3. HDAC8 localization and function

In 2000, the localization of HDAC8 was described predominantly nuclear by Hu et al., using cDNA transfection coupled with immunofluorescence assays (Hu et al., 2000). Nevertheless, other studies identified HDAC8 as predominantly cytoplasmic. In contrast to Hu et al., Waltregny D. et al. reported that HDAC8 is predominantly cytosolic in human tissues and *in vitro* grown human vascular smooth muscle cells, where it displays a cytoskeleton-like pattern of expression. They also provided evidence that HDAC8 may co-localize with the smooth muscle cytoskeleton protein α-actin (α-SMA) (Waltregny et al., 2004). Furthermore, they explained that the Hu et al. observation of HDAC8 predominantly in the nucleus could be due to improper folding of the N-terminally tagged protein construct, which may hamper HDAC8 proper location into the cytoplasm (Hu et al., 2000; Waltregny et al., 2004). Indeed, another group has found HDAC8 located in both, the cytoplasm and the nucleus in HEK293 cells transfected with an HDAC8 construct tagged at the C- terminal (Wyngaert et al., 2000). The possibility that HDAC8 may have a changeable location between cytoplasm and nucleus, depending on the cell type and/or possible post-translational modifications, such as phosphorylation cannot be ruled out (Lee, Rezai-Zadeh, and Seto, 2004). It has been suggested that HDAC8 could

have different roles depending on its cellular localization, due to the involvement of the putative HDAC8 substrates in a wide variety of cellular processes, like metabolism, cell differentiation and DNA repair. If so, the localization of HDAC8 can be strongly dependent on the cell lines or the methodology used. However, cell cycle dependent localization was not yet described in cell cycle progression of human cells.

The HDAC8 function has been involved in many processes mainly depending on the histone and/or non-histone substrates. The entry into the cell of any virus is controlled by a thorough process involving several proteins. HDAC8 is one of those proteins promoting the productive entry of Influenza A virus (IAV) into tissue culture cells by enhancing endocytosis, acidification, and penetration of the incoming virus as Yamauchi et al. explained. The HDAC8 effects relate to dramatic alterations in the organization of the microtubule system, and, consequently, a change in the behavior of the late endosomes and lysosomes. The HDAC8 depletion resulted in a loss of centrosome-associated microtubules affecting late penetrating enveloped viruses since the HDAC8 depletion prompted the inhibition of infection by the Uukuniemi virus. Establishing that HDAC8 is a powerful regulator of microtubule organization, centrosome function, endosome maturation, and infection by IAV or other late penetrating viruses (Yamauchi et al., 2011). The vital role of the HDAC8 enzyme is also found in schistosomiasis parasitic disease (by Schistosoma sp. or Flatworm). Therefore, HDAC8 can be targeted to combat schistosomiasis (Marek et al., 2013). In Cornelia de Lange syndrome (CdLS), an abnormal enzymatic activity of HDAC8 has been identified as the cause of that disorder. Deardorff and co-workers identified HDAC8 as deacetylase of SMC3. The SMC3 is a subunit of the cohesin complex which mediates the correct segregation of sister chromatids to the opposite poles during mitosis or meiosis. The loss of HDAC8 activity leads to the accumulation of acetylated SMC3. This accumulation precludes the proper dissolution of pro-cohesive elements which are necessary for the recycling of ‘refreshed’ cohesin for the next cell cycle, which results in decreased cohesin at localized sites, causing both cellular and clinical features of CdLS (Deardorff, Bando, et al., 2012). That pathway is detailed explored in the topic *“Implications in Cornelia de Lange Syndrome "* (next section 1.1.4). A critical role for HDAC8 affecting the smooth muscle contraction at the tissue level has been identified. HDAC8 is responsible for the regulation of the cortactin deacetylation in smooth muscle. That deacetylated cortactin promotes actin polymerization and smooth muscle contraction. In addition, the HDAC8 inhibition induces relaxation of smooth muscle (Li et al., 2014). Recently, a relationship between HDAC8 and cilia assembly and elongation were identified. The depletion of

HDAC8 significantly reduced the number of cells with cilia and the ciliary length. That showed a positive correlation between the cilia assembly and cellular levels of HDAC8, suggesting the HDAC8 directly participated in cilia assembly (Park et al., 2019). In mice oocytes, Hdac8 is being reported as crucial for female fertility. Defects in oogenesis that result in smaller fully grown oocytes with a reduced ability to resume meiosis were observed in Hdac8- knocked out prior to pre-meiotic S phase and cohesion establishment oocytes. These suggested that the expression of the deacetylase Hdac8 is required early in oogenesis for optimal fertility (Singh et al., 2019). It should be noted that recent studies in mice oocytes showed that Hdac8 regulates meiotic spindle assembly (Zhang et al., 2017).

The HDAC8 interacts directly or/and indirectly with other substrates, which explain its involvement in cancer pathways. Those are described in the topic "*The role of HDAC8 in oncogenesis*" (next section 1.1.5).

1.1.4. HDAC8 and inherited disorders

1.1.4.1. Implications in Cornelia de Lange Syndrome

Cornelia de Lange Syndrome (CdLS) (OMIM #300882), also known as Brachmann-de Lange syndrome is a severe and rare multisystemic disorder well characterized with an estimated prevalence of about 1:10000 to 1:30000 individuals (Ramos et al., 2015). CdLS was firstly described by Brachmann in 1916 and subsequently by de Lange in 1933 (Brachmann W., 1916; deLangeC., 1933; Verma, Passi, and Gauba, 2010). The clinical presentation includes a broad spectrum of phenotypes characterized by postnatal growth retardation, microcephaly, hearing loss, gastroesophageal reflux, feeding difficulties, cardiac defects, genitourinary anomalies and intellectual disabilities (Kline et al., 2018).

As mentioned above the correct segregation of sister chromatids to the opposite poles during mitosis or meiosis is ensured by a protein complex named cohesin. This complex is important to maintain sister chromatids connected ensuring cell division fidelity (Nasmyth and Haering, 2009). CdLS spectrum disorders are referred to as cohesinopathies since most cases result from genetic defects in cohesion's structure or regulatory proteins, due to pathogenic variants in *NIPBL*, *SMC3* and *RAD21* or in the X-linked genes *SMC1A* and *HDAC8*. The core cohesin proteins are encoded by *SMC1A*, *SMC3* and *RAD21*, whereas regulatory are encoded by *NIPBL* and *HDAC8* (Deardorff, Bando, et al., 2012; Ünal et al., 2008). *NIPBL* pathogenetic variants are responsible for about 60% of patients with CdLS. Only 5-10% of the CdLS patients have pathogenetic

variants in *SMC1A*, *SMC3*, *RAD21,* or *HDAC8* genes (Deardorff et al., 2007; Deardorff, Bando, et al., 2012; Deardorff, Wilde, et al., 2012; Krantz et al., 2004; Mannini et al., 2013; Tonkin et al., 2004). Importantly, 30% of CdLS patients have no gene associated with pathophysiology suggesting that there is a considerable number of players not yet identified.

The cohesin complex is composed of two Structural Maintenance of Chromosomes proteins (SMC1A and SMC3) and two non-SMC subunits (RAD21, STAG1/2) (Nasmyth and Haering, 2009) (Figure 4A). SMC3 acetylation and deacetylation are essential for the cohesin function. The SMC3 subunit is acetylated by ESCO1/2 during S phase to establish cohesion between replicated chromosomes (Figure 4A) (Ben-shahar et al., 2008; Heidinger-Pauli, Ünal, and Koshland, 2009; Ünal et al., 2008). Lately, at anaphase, acetylated SMC3 is deacetylated by HDAC8. Deacetylation of SMC3 leads to cohesin complex release from chromatin and that is crucial to the correct segregation of the sister chromatids to the opposite poles and for the recycling of cohesin for use in subsequent cell cycles (Figure 4B) (Deardorff, Bando, et al., 2012; Deardorff, Porter, and Christianson, 2016).

Deardorff et al. showed that mutation or depletion of HDAC8 led to the accumulation of ac-SMC3, consequently, an inefficient dissolution of the ‘used’ cohesin complex released from chromatin in anaphase was observed. Furthermore, loss-of-function mutation (nonsense or missense) in the *HDAC8* gene was observed in CdLS children (Deardorff, Bando, et al., 2012). In summary, the HDAC8 plays a key role in cohesin function and consequently is essential for cohesin deacetylation and recycling for the next cell cycle.

1.1.4.2. HDAC8 affected individuals

To date, 45 *HDAC8* variants were predicted and reported in ClinVar database, to be associated with CdLS. Sixteen of those were reported as pathogenic (red circles), seventeen as likely pathogenic (blue circles), one as benign (grey circles), one as likely benign (black circles), eight with uncertain significance (yellow circles), and two with conflicting interpretations of pathogenicity (green circles). *HDAC8* variants in bold are those supported by published affected individuals diagnosed with CdLS (OMIM #300882) (Figure 5) (Deardorff, Bando, et al., 2012; Harakalova et al., 2012). Clinically, patients were reported with intellectual disability or cognitive delay, growth retardation, facial dysmorphism, limb anomalies, large fontanels, hearing loss and happy personality. Some features are present just in one case such as hypogonadism, gynecomastia, asymmetric skull, dysplastic kidneys, pulmonary stenosis and atrial septum aneurysm (Table 2) (Deardorff, Bando, et al., 2012; Harakalova et al., 2012). Therefore, it is not clear if these particular characteristics are directly associated with the *HDAC8* mutations or exacerbated by any other gene variant synergism.

In 2014, a research team assessed an international cohort of 586 individuals with features of CdLS and overlapping phenotypes without a genetic cause. Twenty-five out of 585 individuals had loss-of-function mutations in *HDAC8* gene. Many features were similar to those observed in typical CdLS including postnatal growth retardation (28%), microcephaly (29%), hearing loss (59%), gastroesophageal reflux (67%), feeding difficulties (86%), cardiac defects (36%), genitourinary anomalies (44%), and intellectual disabilities (100%). Craniofacial features were also common, such as brachycephaly (70%), arched eyebrows (88%), synophrys (90%), long eyelashes (45%), depressed nasal bridge (45%), anteverted nares (76%), long philtrum (57%), downturned corners of the mouth (57%), small widely spaced teeth (61%), micrognathia (59%) and cleft palate without cleft lip (18%). Most patients also had small hands and feet. Unique features not seen in typical CdLS included delayed fontanel closure (50%), ocular hypertelorism (47%) and/or telecanthus (64%), hooding of the upper eyelids (46%), bulbous nasal tip (66%), dental anomalies (50%), and nevus flammeus (58%) (Kaiser et al., 2014).

Dosage dependent inactivation of X chromosome in females is mediated by a well described mechanism as mentioned above in 1.1.1. If this mechanism fails, the mutant allele is not completely inactivated and the carrier of pathogenic *HDAC8* mutants may develop a clinical phenotype. Diagnosis of HDAC8 patients is very complex because the severity of the phenotypes correlates not only with each variant but also with the

percentage of the expression of the mutated allele in each patient. This explains the wide spectrum of clinical features described (Table 2) and the difficulties inherent to the establishment of the pathogenicity of some variants (Figure 5).

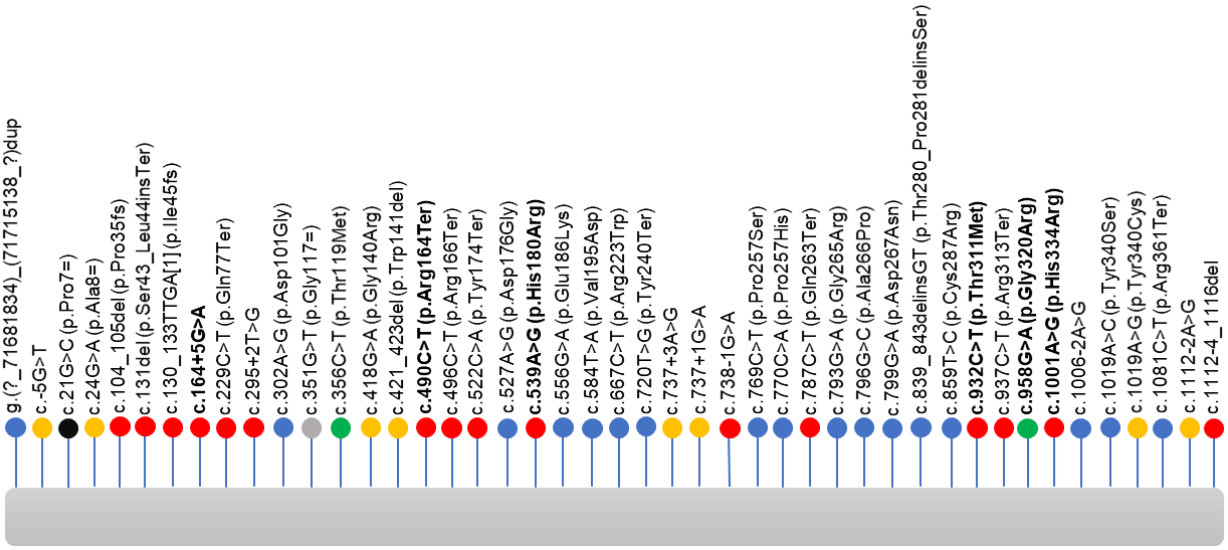

Figure 5 *HDAC8* variants associated with CdLS reported in ClinVar (not at scale).

Circles with different colors represent the clinical condition: Pathogenic variants (red circles), likely pathogenic (blue circles), benign (grey circles), likely benign (black circles), uncertain significance (yellow circles) and conflicting interpretations of pathogenicity (green circles).

Table 2 Clinical features of CdLS patients with *HDAC8*pathogenic variants.

Grey rectangles represent the common features to all cases (Adapted from Deardorff et al., 2012).

	***HDAC8* variant**					
Clinical feautures	c.164+5G>A	c.490C>T (p.Arg164Ter)	c.539A>G (p.His180Arg)	c.932C>T (p.Thr311Met)	c.958G>A (p.Gly320Arg)	c.1001A>G (p.His334Arg)
Intellectual disability or cognitive delays	X	X	X	X	X	X
Facial dysmorfism	X	X	X	X	X	X
Grow th retardation	X	X	X	X	X	X
Large fontanels				X	X	X
Limb length discrepancies		X				X
Hearing loss				X	X	
Happy personality					X	X
Hypogonadism	X					
Gynecomastia	X					
Asymmetric skull		X				
Dysplastic kidneys		X				
Pulmonary stenosis				X		
Atrial septum aneurysm					X	

1.1.5. Role of HDAC8 in oncogenesis

HDAC8, when deregulated, is responsible for different types of cancer such as lung, ovarian, prostate, hepatocellular carcinoma, pancreatic, colon, and breast, acute lymphocytic leukemia (ALL) and acute myeloid leukemia (AML) along with childhood neuroblastoma. The deregulation of HDAC8 expression or interaction with different transcription factors explains the wide range of cancers making this gene an attractive anticancer target.

To date, several works reported the importance of HDAC8 as a cancer driver. For example, in invasive breast tumor cells HDAC8 is upregulated and correlates with invasiveness (Park et al., 2011). In gastric cancer and hepatocellular carcinoma, the upregulation of HDAC8 promotes proliferation and inhibits apoptosis (Chakrabarti et al., 2015; Song et al., 2015; Wu et al., 2013; Yan et al., 2013). In invasive breast tumor cells, the upregulation of HDAC8 results in overexpression of HDAC1 and HDAC6 to promote invasion (Park et al., 2011). In human colon, gastric adenocarcinoma, prostate, lung, colon, neuroblastoma, leukemia, and cervical cancer cell lines were shown that HDAC8 knockdown inhibits cell proliferation (Higuchi et al., 2013; Oehme et al., 2009; Song et al., 2015; Vannini et al., 2004).

In 2008, a research team described the characterization of a novel HDAC8-selective inhibitor, PCI-34051. The inhibition of HDAC8 enzymatic activity using PCI-34051 inhibits cell growth and induces apoptosis in cell lines derived from T-cell lymphomas or leukemias, but not in other hematopoietic or solid tumor lines. This suggests that HDAC8 enzymatic inhibition might be a beneficial treatment for T-cell-derived malignancies (Balasubramanian et al., 2008). It was also tested on ATL cell lines and revealed to be highly effective by significantly suppressed cell growth (Higuchi et al., 2013).

To date, several mechanisms of action were described for HDAC8. It has been associated with genes and proteins involved in cancer such as inv(16) fusion protein, telomerase protein, tumor suppressors *P53* gene and p73 protein, SOCS1/3 and *BMF.*

In acute myeloid leukemia-1 HDAC8 has been identified associated with the chromosomal translocation inv(16) fusion protein, acting both as deacetylase and interacting scaffold (Liu et al., 1993). That fusion protein cooperates with AML1 to repress the transcription of AML1-regulated genes (such as *p21*), representing 8% of acute myeloid leukemia-1 (AML-1) (Mitelman and Heim, 1992). HDAC8 binding domains interact with the inv(16) fusion protein to repress transcription targets controlling inv(16)-mediated repression (Qi et al., 2015).

The maintenance of telomere (genomic) stability is crucial to avoid tumorigenesis. The telomerase activity has been shown to be affected by HDAC8. That protects the human ever-shorter telomeres 1B (hEST1B) protein against ubiquitin-mediated degradation through a phosphorylation function-dependent process (Lee et al., 2006).

The enhanced transcription of *P53* has been associated with the ectopic expression of HDAC8. The inhibition/ knockdown of HDAC8 has been shown to be more effective in tumor cells harboring a *P53* mutation. Moreover, HDAC8 knockdown leads to an increased expression and acetylation of p53 protein in HCC cells resulting in a decrease of cell proliferation and enhancement of the apoptosis rate *in vitro*. HDAC8 is also involved in the regulation of another transcription factor of the p53 family, p73. The p73 also plays an important role in many biological processes, such as neuronal development and tumorigenesis (Killick et al., 2011). HDAC8 upregulates the p73 expression by cooperating with the transcription factor differentiated embryo-chondrocyte expressed gene 1 (DEC1), thus differentially controlling the p73 tumor suppressor (Qian et al., 2014).

Downregulation of cytokine signaling 1/3 (SOCS1/3) suppressor has been associated with HDAC8 in cancer. The HDAC8 inhibition prompt to SOCS1/3-dependent reduction of cell proliferation along with the suppression of hematopoietic cell activity in myeloproliferative neoplasms (Gao et al., 2013).

Additionally, in colon cancer, *BMF* gene (a Bcl-2-modifying factor involved in apoptosis activation) has been identified to be a direct target gene of HDAC8 repression associating and cooperating with STAT3 to repress *BMF* transcription. The regulation of *BMF* by HDAC8-STAT3 has a crucial role in cellular apoptosis and cell proliferation (Kang et al., 2014).

The regulation of MAPK and JUN signaling in BRAF-mutant melanoma has been directly associated with HDAC8. The deacetylation in melanoma of c-Jun by HDAC8 increases MAPK activity. Furthermore, proteomic data obtained using STRING analysis demonstrated that HDAC8 is involved in a wide range of cellular processes such as cell cycle regulation, RNA binding, ERK signaling, ribosomal function and organization of the cytoskeleton (Emmons et al., 2019). HDAC8 was also reported to be a player in chemotherapy resistance using some DNA based alkylating agents. The knockdown of HDAC8 leads to decreased levels of O^6-methyl-guanine DNA methyltransferase (MGMT), a DNA damage repair enzyme, in glioblastoma multiforme cell lines reverting its chemosensitivity (Santos-Barriopedro et al., 2019).

Recently it was reported a direct interaction between HDAC8 and SMAD4. HDAC8 acts as a linker in the SMAD3/4/HDAC8 complex, and that complex occupies SIRT7 promoter suppressing SIRT7 transcription. The decrease of SIRT7 activates TGF-β signaling involved in multiple cellular processes, such as cell growth, stemness, migration and invasion (Muraoka et al., 2002). Treatment with HDAC8 inhibitor compromises TGF-β signaling via SIRT7-SMAD4 and consequently, inhibits breast cancer metastasis and improves chemotherapy efficacy (Tang et al., 2020).

It has also been described that HDAC8 interacts with AKT1 to decrease its acetylation while increasing its phosphorylation. In addition, the HDAC8 could decrease the GSK-3β expression by increasing its Ser9-phosphorylation, which leads to increased protein stability of Snail, an important regulator of epithelial-mesenchymal transition (EMT). Furthermore, the HDAC8/Snail axis acted as an adverse prognosis factor for *in vivo* progression and overall survival rate of breast cancer patients. This study concluded that HDAC8 can trigger the dissemination of breast cancer cells via AKT/GSK-3β/Snail signals (An et al., 2020).

In summary, it is important to dissect the exact function of HDAC8 and its substrates in the cell cycle to understand their cellular role in tumorigenesis. Being HDAC8 a protein linked to a wide range of different cancer and complex canonical biochemical pathways, it is important to identify all interacting players and fully understand their role to uncover his importance in tumorigenesis.

1.1.6. Mitosis

Mitosis is a short period in the cell cycle in which one cell divides into two genetically identical daughter cells. To reproduce themselves, cells need to duplicate their genetic material to give rise to two genetically identical daughter cells. In multicellular species, cell division is essential to make a new individual and to replace cells in an adult body.

Walther Flemming is considered the pioneer of mitosis research, being the first investigator to name the process as Mitosis. Flemming divided mitosis into two parts: the progressive phase (chromosomes are condensed and aligned at the center of the spindle) and the regressive phase (separation of the sister chromatids) (Figure 6) (Paweletz, 2001).

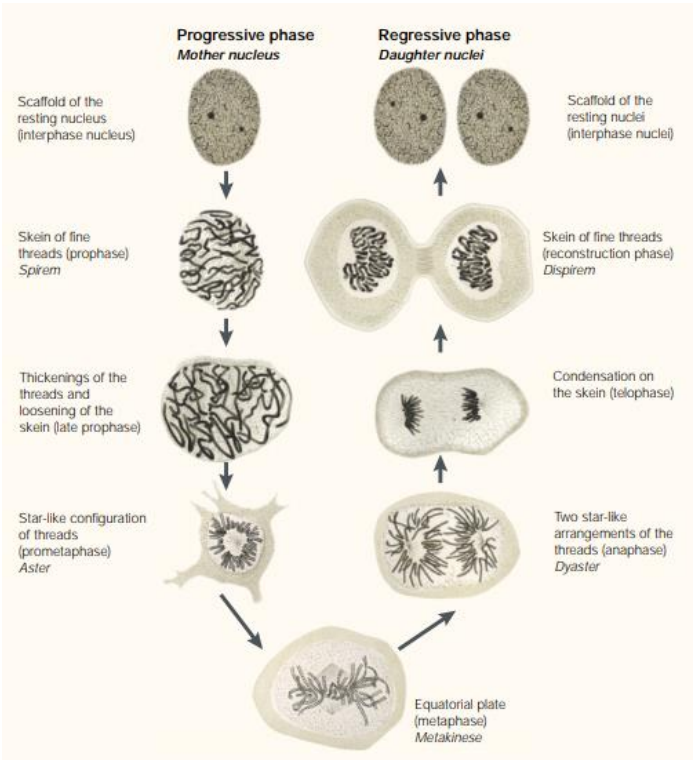

Figure 6 Flemming's Mitosis.

Mitosis is divided into two parts: the progressive phase, constituted by prophase, prometaphase, and metaphase; the regressive phase that starts in the metaphase to anaphase transition and finishes with telophase (Adapted from Paweletz, 2001).

The cell cycle is divided in the following stages: G1 (Gap 1), S (Synthesis), G2 (Gap 2), and M (Mitosis). The first three stages together compose the Interphase (Cooper and Hausman, 2000). The M phase can be considered as the phase that includes Mitosis itself (the division of the nuclear content) and Cytokinesis (the division of the cytoplasmic content into two separated daughter cells). Mitosis, by its own, can be divided in the following main stages: prophase, prometaphase, metaphase, anaphase, and telophase (O'Connor, 2008). During prophase chromosomes start to condense. Sister chromatids are bound to each other by a specialized structure of the chromosome named centromere. Next, microtubules (MTs) emerge from the two centrosomes and enter in a process of search-and-capture of a multiprotein structure that forms at the chromosome's centromere, the kinetochore The connected microtubules are called kinetochore microtubules (KT-MTs), and together with the remained non-kinetochore microtubules form the structure known as the mitotic spindle (Rieder, 1982). This stage is named

prometaphase. After the establishment of the KT-MT attachments, the MTs begin to pull and push the chromosomes to the equatorial plate of the cell, resulting in their alignment and to the formation of the metaphase plate (Kapoor et al., 2006; Rieder and Salmon, 1998). When the cell enters anaphase, the connections that bind the two sister chromatids composed by cohesin are cleaved (Uhlmann, Lottspelch, and Nasmyth, 1999). Then the shortening of the KT-MTs pulls the sister chromatids to the two opposite poles of the cell. In telophase, the nuclear envelope reforms at each daughter cell and surrounds the new daughter chromosomes, which start to decondensate leading to the reappearing of the nucleus. The separation of cytoplasm then occurs, with the definition of the cytokinetic, resulting into two separated daughter cells with identical genetic composition of the mother cell (Glotzer, 2001).

1.1.6.1. Mitotic fidelity and genomic instability

The major goal of mitotic fidelity is ensuring the accurate distribution of the genetic material between the two daughter cells. During mitosis, both the correct segregation of newly duplicated chromosomes and the proper positioning of daughter cells, require an elegant mitotic apparatus and complex microtubule-based protein machinery organized in a bipolar manner (Bloom, 2004). The assembly of the mitotic apparatus occurs *de novo* once per cell cycle and requires a high level of cooperation between MTs, centrosomes, microtubule-associated proteins, and molecular motors (Bloom, 2004; Schnerch and Nigg, 2016).

The MTs are one of the necessary components to ensure the accurate assembly of the mitotic apparatus. That are assemblies of α- and β-tubulin heterodimers that are arranged in a head-to-tail manner into protofilaments. The γ-tubulin is responsible for MTs nucleation (Kollman et al., 2011; Meunier and Vernos, 2012).

Errors during mitosis, including defects in the spindle assembly, sister chromatid cohesion, and kinetochore-microtubule attachments can lead to: anaphase lagging chromosomes- chromosomes that lag behind at the spindle equator while all the other chromosomes move toward the spindle poles, chromatin bridges- chromosomes whose chromatids cannot separate from each other, and chromosome congression failure- chromosomes fail to align during the process of chromosome congression to the metaphase plate. Such abnormalities compromise mitotic fidelity and consequently lead to aneuploidy and that are a major cause of birth anomalies and a hallmark of

tumorigenesis (Bloom, 2004; Ried et al., 2012; Schnerch and Nigg, 2016; Yang et al., 2002).

Some class I HDACs have been associated with mitosis, ensuring mitotic fidelity. For example, HDAC3 knockdown resulted in a collapsed mitotic spindle with impaired KT-MTs attachments, suggesting that class I HDACs is involved in the regulation of spindle formation and KT-MTs attachments (Ishii et al., 2008). Furthermore, it was reported that the loss of HDAC1 and 2 led to an increased mitotic defect, chromatin bridges, and micronuclei, suggesting that deacetylases are necessary for accurate chromosome segregation (Jamaladdin et al., 2014). Additionally, a class II HDAC, HDAC6, was reported to co-localize with mitotic spindle in metaphase and with y-tubulin. During telophase, HDAC6 is enriched in the center of the midbody. Suggesting that HDAC6 might play a role in mitosis participating in microtubules organization (Zhang et al., 2003).

The role of HDAC8 in the maintenance of mitotic fidelity in human cells was not yet described. So far, research studies have been shown that HDAC8 is required for centrosome cohesion and MT organization. Disorganization of MT and consequently random orientation in the cytoplasm are observed in HDAC8 depleted cells. The centrosomes staining revealed that instead of exhibiting two closely paired spots in the microtubule organization center (MTOC), they appeared in similar spots that were far apart, and occasionally on opposite sides of the nucleus. Consequently, a higher percentage of centrosome splitting in HDAC8 depleted cells was detected (Yamauchi et al., 2011). Interestingly, the α-tubulin has been described as a novel interacting partner of HDAC8. The HDAC8 binds and deacetylates the α-tubulin at ac-lys40, a residue only present in α-tubulin. It was observed an increase of acetylated α-tubulin expression by HDAC8 knockdown or inhibition, which in turn stabilizes the microtubules and inhibits cell migration and mitotic entry in cervical cancer HeLa cells (Vanaja, Ramulu, and Kalle, 2018).

Zhang et al. identified that Hdac8 protein localizes at spindle poles and positively participates in the regulation of microtubule organization and spindle assembly in mouse oocyte meiosis. After depletion of Hdac8 during oocyte meiotic maturation chromosome misalignment, spindle defects, and impaired KT-MTs attachments were observed. Those anomalies consequently led to a higher incidence of aneuploidy in Hdac8-depleted eggs. The same results were observed when Hdac8 activity was inhibited. Moreover, the authors highlight that Hdac8 is necessary for the correct localization of γ-tubulin to the spindle poles. Overall, the Hdac8 plays a significant role in regulating spindle assembly and thus ensuring the ploidy in mouse eggs (Zhang et al., 2017). Those works revealed

that HDAC8 has a role in mitosis or in mitotic components. To the best of our knowledge, no studies were conducted in order to investigate the mitotic fidelity in somatic human cells.

Over the years, HDAC8 has been implicated in a vast number of disorders such as neurodegenerative disease (CdLS-5) and cancer (Figure 7). Yet, the involvement of HDAC8 in the maintenance of mitotic fidelity and consequently a possible enrollment to aneuploidy predisposition is poorly explored.

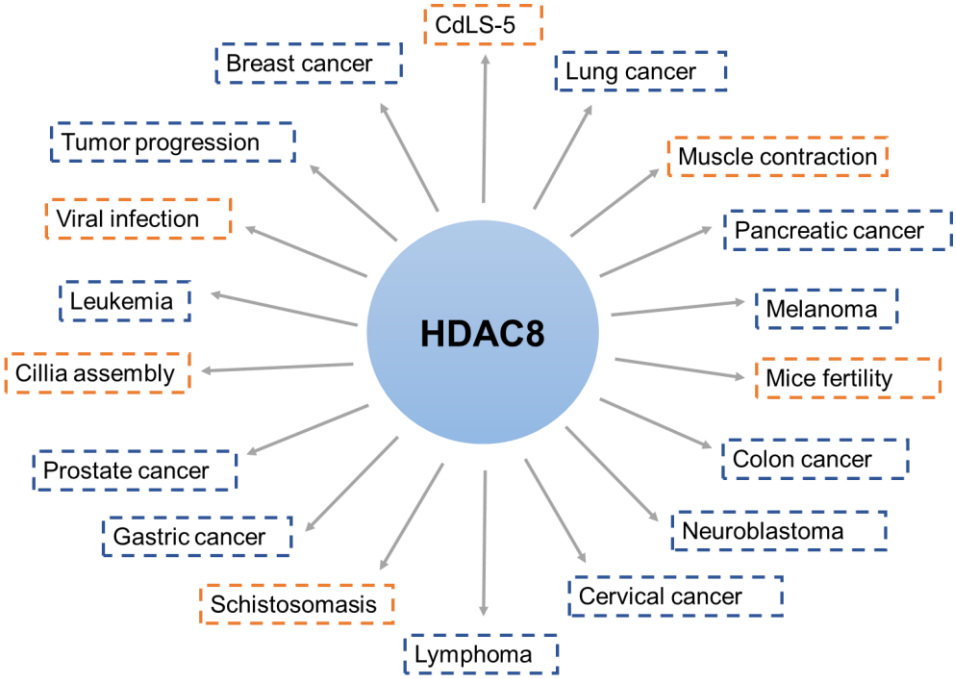

Figure 7 HDAC8 associated phenotypes.

Phenotypes without cancer association (orange rectangles), phenotypes with cancer association (blue rectangles). CdLS-5: Cornelia de Lange Syndrome type 5.

Author's note: *These studies were conducted during the covid-19 pandemic. The first aim of this master thesis was to dissect the role of HDAC8 and its Network of Interacting Partners in the maintenance of mitotic fidelity, but experimental limitations due to pandemic confinement forced us to make some changes to the tasks initially proposed.*

AIM OF THE STUDY

To date, the role of HDAC8 in mitotic fidelity is not fully understood. The aim of this work is to investigate the involvement of HDAC8 in the maintenance of mitotic fidelity. Peripheral blood, fibroblasts, and human-derived lymphoblastoid cell lines – EBV transfected (LCLs) samples from a clinically CdLS-like case carrying a mutant *HDAC8* allele were used. Exploring HDAC8 function will provide insights into the mechanisms behind *HDAC8*-related disorders such as tumorigenesis, a well-known result of genomic instability. Importantly, this work will provide new insights towards the variant pathogenicity.

Specific goals:

- To describe HDAC8 location on different stages of the cell cycle.
- To investigate the HDAC8 function in mitotic fidelity using siRNAs.
- To analyze the impact of the mutant *HDAC8* allele in chromosome instability, and its expression.

The tasks of this master's degree project were conducted in three Institutions, Centro de Genética Médica Doutor Jacinto Magalhães (CGMJM), under the supervision of Drª Paula Jorge and Nuno Maia, Instituto de Inovação e Investigação (i3S), under the supervision of Drª Ariana and Instituto de Ciência Biomédicas Abel Salazar (ICBAS), under the supervision of Drª Beatriz Porto and Claudia Oliveira.

MATERIAL AND METHODS

1. Material

1.1. Cell lines

i. HeLa WT
ii. Peripheral blood
iii. Fibroblasts
iv. Epstein-Barr virus (EBV) transformed human B lymphocytes; or human B lymphoblastoid cells (LCLs)

1.2. Growth Media

Different cell lines required different growth conditions.

i. HeLa cell lines
   Dulbecco's Modified Eagle's Medium (DMEM; Gibco™, Thermo Fisher, Waltham, Massachusetts, USA)
   5% or 10% Fetal bovine serum (FBS; Gibco™)

ii. Peripheral blood
   Roswell Park Memorial Institute-1640 (RPMI-1640; Sigma-Aldrich®, St. Louis, Missouri, USA)
   15% Fetal bovine serum (FBS; Gibco™)
   1% Penicillin/Streptomycin (Pen/Strep; Gibco™)
   29 mg/mL of L-glutamine (Sigma-Aldrich®)
   5 µg/mL of phytohemagglutinin (Gibco™)

iii. Fibroblasts
   Dulbecco's Modified Eagle's Medium (DMEM; Gibco™)
   15% Fetal bovine serum (FBS; Gibco™)
   1% Penicillin/Streptomycin (Pen/Strep; LONZA®, Basel, Switzerland)

iv. Human-derived lymphoblastoid cell lines (LCLs)

Roswell Park Memorial Institute-1640 (RPMI-1640; Sigma-Aldrich®)

15% Fetal bovine serum (FBS; Gibco™)

1% Penicillin/Streptomycin (Pen/Strep; LONZA®)

1.3. Buffers, solutions, and reagents

All buffers and solutions were prepared with demineralized water and, if necessary, filter sterilized or autoclaved for long-term storage.

1.3.1. Buffers and solutions for transfection, immunofluorescence and western blotting

***HDAC8* siRNA HeLa cells transfection reagent:**

i. Lipofectamine RNAiMax (Invitrogen™) diluted in Opti-MEM (Gibco™)

Immunofluorescence studies:

i. Phosphate Buffered Saline (PBS) Buffer, pH 7.5 (Autoclaved)

50 mM $NaPO_4$

150 mM NaCl

ii. Phosphatase Buffered Saline- Tween20 (PBS-T) Buffer

50 mM $NaPO_4$

150 mM NaCl

0.1% (v/v) Tween20

iii. Paraformaldehyde 4% diluted in PBS

iv. Triton-X 100 0.5% diluted in PBS

v. Mounting Medium

20 mM Tris pH 8

0.5 mM N-propyl gallate

90% glycerol

Western blotting:

i. Lysis Buffer NP-40 solution

20 mM HEPES/KOH
1 mM EDTA
1 mM EGTA
150 mM NaCl
0.5% NP-40
10% glycerol
2 mM DTT at -20°C
Protease inhibitor 4C+PMSF 0.1 mM at -20°C 1:100, pH 7.9

ii. Sample Buffer

50 mM Tris-HCl pH 6.8
2% SDS
10% glycerol
1% β-mercaptoethanol
12.5 mM EDTA
0.02% bromophenol blue

iii. Gel Running Buffer

25 mM Tris
192 mM Glycine
0.1% (w/v) SDS

iv. Blotting Buffer

48 mM Tris
39 mM Glycine
0.037% (w/v) SDS
20% (v/v) Methanol

v. Ponceau S

0.2% Ponceau S
3% Trichloroacetic acid (TCA)

vi. Enhanced Chemiluminesence (ECL) Solution

125 mM 3-Aminophtelhydrazide
45 mM 4-Hydroxycinnamic acid
100 mM Tris- HCL, pH 8.5
0.001845% H_2O_2

1.3.2. Solutions/Reagents in chromosome analysis

Chromosome instability and cell ploidy analyses were performed at the Cytogenetics Laboratory, ICBAS-UP. Chromosome analysis was carried out in peripheral blood, fibroblasts, and LCLs samples (see Table 3 for solutions and reagents used):

Table 3 Solutions and reagents used in chromosome analysis.

Solutions/Reagents	Function	Stock concentration	Final concentration	Source
1,3-Butadiene diepoxide (DEB)	DNA crosslinking agent used to induce DNA damage and chromosome breakage.	1.0796 g/mL	0.005 µg/mL and 0.01 µg/mL diluted in RPMI for LCLs and fibroblasts, and 0.05 µg/mL and 0.1 µg/mL peripheral blood.	Sigma-Aldrich®
Colcemid	Solution used to depolymerize microtubules inhibiting the spindle poles formation and blocks mitosis at metaphase.	10 µg/mL	0.125 µg/mL	Gibco™
Trypsin-EDTA (1X)	Used to detach the fibroblasts	0.05%	0.05%	Gibco™
Potassium chloride (KCl)	Hypotonic solution used to disrupt the cellular membrane	1 M	0.05 M for fibroblasts, and 0.075 M for LCLs and peripheral blood	Merck™, Darmstadt, Germany
Methanol:Acetic acid	Fixative solution. Used to fix cells.	Methanol 99.8% of purity and Acetic acid 99.7% of purity	Proportion 3:1	Fisher Chemical™, Waltham, Massachusetts, USA
Giemsa	Dye used to stain the chromosomes		3% in distilled H_2O	Merck™

1.4. Antibodies

Tables 4 to 8 describe the antibodies used in immunofluorescence and other studies.

Table 4 HDAC8 primary antibodies.

Antibody	Species	Final concentration (µg/mL)	Source
Anti-HDAC8 (F-9)	Mouse	1 µg/mL	Santa Cruz Biotechnology®, Dallas, Texas, USA (SC-374180)

Table 5 Tubulin primary antibody.

Antibody	Species	Dilution	Source
Anti-α-tubulin	Rat	1:500	Bio-Rad, Hercules, CA, USA (MCA77G)

Table 6 Kinetochore antibody.

Antibody	Species	Dilution	Source
Human anti-CREST	Human	1:1000	Abyntek®, Derio, Vizcaya, Spain

Table 7 DNA staining.

DNA staining	Dilution	Source
DAPI	1:100000	Sigma-Aldrich®

Table 8 Secondary antibodies.

Antibody	Dilution	Source
Alexa Fluor™ anti-Mouse 488	1:500	Invitrogen™, Carlsbad, CA, USA
Anti-Rabbit 568	1:500	Invitrogen™
Anti-Human 647	1:500	Invitrogen™
Anti-Rat 568	1:250	Invitrogen™

1.5. Primers

Table 9 *HDAC8* siRNA and Scramble siRNA primers.

Primer name	Sequence 5' → 3'	Final concentration (nM)	Source
HDAC8 siRNA	GGUCCCGGUUUAUAUCUAUtt	25 nM	Ambion®, Invitrogen™ (s31698)
Scramble siRNA	CUUCCUCUCUUUCUCUCCCUUGUGA	25 nM	Invitrogen™

Table 10 cDNA *HDAC8* primers.

Primer name	Sequence 5' → 3'	Source
cDNA_*HDAC8*-F	CAGGTGACGTGTCTGATGTTG	Ambion®, Invitrogen™,
cDNA_*HDAC8*-R	ACCCCGGTCAAGTATGTCC	Ambion®, Invitrogen™,

Table 11 Human androgen receptor methylation assay (HUMARA) primers.

Primer name	Sequence 5' → 3'	Source
HUMARA-F	TCCAGAATCTGTTCCAGAGCGTGC	Thermo Fisher
HUMARA-R	GCTGTGAAGGTTGCTGTTCCTCAT	Thermo Fisher

1.6. Endonucleases

Table 12 Endonuclease cutting region.

Enzyme name	Cutting region	Source
*Hha*I	5'… G C G C …3' 3'… C G C G …5'	New England BioLabs®, Ipswich, Massachusetts, USA
*Rsa*I	5'… G T A C …3' 3'… C A T G …5'	New England BioLabs®

2. Methods

2.1. Thawing the frozen cells

HeLa, fibroblasts, and lymphoblastoid cell lines had been previously stored in cryovials at -80ºC. The stored cryovials were transferred to a 37ºC water bath or to the humidified incubator at 37ºC. After thawing, cells were transferred into a 15 mL Falcon tubes and diluted with approximately 7 mL of medium (DMEM, Gibco™ or RPMI, Sigma-Aldrich®), depending on the cell type. The Falcon tubes were centrifuged 10 minutes at 352 g, then the supernatant was removed- this is an important step to remove DMSO, a toxic agent to the cells used for cryopreservation- and re-suspended in 5 mL of DMEM or RPMI supplemented with 10 or 15% of FBS (Gibco™) and 1% of Penicillin/Streptomycin (Sigma-Aldrich® or LONZA®), depending on the cell type. Finally, cell suspension was transferred to T25 flasks and incubated at 37°C in a 5% CO_2, humidified atmosphere.

2.2. Cell line maintenance

2.2.1. HeLa cells

HeLa cells were maintained under Biosafety Level 2 tissue culture standard procedures. Cells were grown in T25 flasks and maintained in DMEM (Gibco™) supplemented with 10% of FBS (Gibco™) at 37°C in a 5% CO_2, humidified atmosphere, until they reached necessary confluence. To detach from the flask surface, cells were treated with 1 mL of Trypsin-EDTA 0.05% (Gibco™) and then incubated 5 minutes at 37ºC. Trypsin was neutralized by the addition of DMEM supplemented with 10% FBS in

a proportion of 1:2. Cells were counted using a hemocytometer (Neubauer cell chamber). Then, were transferred into 6 well-plates, each well containing $0.3x10^6$ cells diluted in 1.5 mL DMEM with 10% of FBS and maintained at the conditions mentioned before. Approximately 24 hours after plating cells were manipulated according to the subsequent study.

2.2.2. Peripheral blood cells

Peripheral blood cells were maintained under Biosafety Level 2 tissue culture standard procedures. Peripheral blood was cultured in RPMI-1640 (Sigma-Aldrich®), supplemented with 15% FBS (Gibco™), 1% of Penicillin/Streptomycin (LONZA®), and 29 mg/mL of L-glutamine (Sigma-Aldrich®). Cultures were stimulated using 5 µg/mL of phytohemagglutinin (Gibco™) and placed in an incubator at 37°C with 5% CO_2, humified atmosphere, for 72 hours. Finally, cells were manipulated following the protocol described in section 2.6.

2.2.3. Fibroblasts

Fibroblasts were maintained under Biosafety Level 2 tissue culture standard procedures. Briefly, cells were grown in T25 flasks and maintained in DMEM (Gibco™), supplemented with 15% of FBS (Gibco™) and 1% of Penicillin/Streptomycin (Gibco™), at 37°C in a 5% CO_2, humidified atmosphere. When approximately 60% confluence was reached, cells were manipulated for chromosome spreads analysis (section 2.6). Aliquots were stored at -80°C after collection of cell suspension into a 15 mL Falcon tubes and centrifuged 10 minutes at 352 g. Pellet was re-suspended in RPMI or DMEM with 7.5% of Dimethyl Sulfoxide (DMSO; Sigma-Aldrich®), to achieve a suspension with $1x10^6$ cells/mL. Finally, the cryovials, after proper label, were stored in Mr. Frosty for 24 hours and then stored at -80ºC.

2.2.4. Lymphoblastoid cells

LCLs were maintained under Biosafety Level 2 tissue culture standard procedures. Cells were grown in T25 flasks and maintained in RPMI (Sigma-Aldrich®) supplemented with 15% of FBS (Gibco™) and 1% of Penicillin/Streptomycin (Gibco™) at 37°C in a 5% CO_2, humidified atmosphere. When approximately 90-95% confluence was reached, cells were manipulated for chromosome spreads analysis (section 2.6). Aliquots were stored at -80°C. Cell pellets were obtained after collection of cell suspension into a 15

mL Falcon tubes and centrifuged 10 minutes at 352 g. Pellet was re-suspended in RPMI or DMEM with 7.5% of Dimethyl Sulfoxide (DMSO; Sigma-Aldrich®), to achieve a suspension with $1x10^6$ cells/mL. Finally, the cryovials properly labeled were stored in Mr. Frosty for 24 hours and stored at -80ºC.

2.3. siRNA experiments

The siRNA experiments were performed in 6-well plates containing glass coverslips, each well containing $1.6x10^5$ cells in 2 mL of DMEM (Gibco™) supplemented with 5% of FBS (Gibco™). A solution containing 5 µL of Lipofectamine™ RNAiMax (Invitrogen™) diluted in 250 µL Opti-MEM (Gibco™) was mixed with 25 nM of *HDAC8* siRNA (Sigma-Aldrich®) diluted in Opti-MEM. On same time, to use as control, other solution containing 5 µL of Lipofectamine™ RNAiMax (Invitrogen™) diluted in 250 µL Opti-MEM (Gibco™) mixed with 25 nM of siScramble (Sigma-Aldrich®) diluted in Opti-MEM was prepared. siRNAs sequences are represented in Table 9. The solutions mix were incubated for 30 minutes at room temperature (RT) and then added dropwise to the well. After an incubation of 6 hours, the medium was removed and replaced with 2 mL of DMEM (Gibco®) with 10% FBS (Gibco™) and incubated for 72 hours in a humidified cell culture incubator at 37ºC and 5% CO_2. To corroborate the specificity of *HDAC8* siRNA depletion, HeLa cells without siRNA transfection, and with Scramble siRNA (targeted random sequences of RNA) were plated.

2.4. Immunofluorescence

Immunofluorescence studies were performed to investigate the localization of HDAC8 and possible effects of its depletion cell cycle progression. After, HeLa cells culturing in 6-well plates and its manipulation. 2 mL of 4% Paraformaldehyde diluted in PBS 1X, or in alternative, 2 mL of 100% Methanol at -20°C, for 10 minutes were used for cell fixation. Coverslips were washed 3 times with PBS 1X. Fixed cells were treated with 2 mL of 0.5% Triton X-100 diluted in PBS 1X for 10 minutes to achieve permeabilization of cell membrane. To block nonspecific signals a blocking solution, PBS with 10% of FBS (Gibco™), for 30 minutes was used. After blocking, the following primary monoclonal antibodies were added to the coverslips: Mouse anti-HDAC8 (Santa Cruz Biotechnology®), Human anti-CREST (Abyntek®), and Rat tyrosinated anti-α-tubulin (Bio-Rad), diluted in PBS Tween20 0.1% with 10% FBS (Gibco™) and incubated overnight at 4ºC. DNA staining was achieved by addition of 4',6-diamidino-2-phenylindole (DAPI; Sigma-Aldrich®) at 1:100000 diluted in PBS Tween20 0.1% with

10% FBS and incubated for 5 minutes at RT. Then, secondary antibodies Alexa Fluor™ anti-Mouse 488 (Invitrogen™), Anti-Rabbit 568 (Invitrogen™), anti-Human 647 (Invitrogen™) and anti-Rat 568 (Invitrogen™) were diluted 1:500, 1:500, 1:500 and 1:250, respectively in PBS Triton X-100 0.1% with 10% FBS, added to the coverslips and incubated for 1 hour, RT. Coverslips were mounted on slides using 20 µL of mounting medium and sealed with nail-polish. Images were produced using a Zeiss Axio Observer Widefield Microscope with 63X objective. Processing of images was made using ImageJ Software.

2.5. Western blotting

Cells were harvested, pelleted by centrifugation at 258 g for 5 minutes, and washed with PBS 1X. Protein extracts were obtained by addition of Lysis Buffer NP-40 solution and frozen in liquid Nitrogen. The suspension was then centrifuged for 5 minutes at 352 g, 4°C, collecting the supernatant. Protein levels were quantified using Bradford Reagent (Thermo Fisher) diluted 1:1 with distilled water, solutions of Bovine Serum Albumin (BSA; Thermo Fisher) with known concentrations, were used as standards. Samples were diluted with distilled water to attain 35 µg of total protein. Sample Buffer was added to the samples and then denatured at 95°C for 5 minutes. The samples were loaded in a 6.5% Acrylamide Gel mounted in a Mini-PROTEAN® vertical electrophoresis apparatus (Bio-Rad). The Protein Marker used was the NZYColour Protein Marker II (NZYTech, Lisbon, Portugal). Gel was placed between blotting buffer soaked three Whatman papers, the nitrocellulose membrane, and three additional Whatman papers. A semi-dry blotting apparatus was used to transfer the proteins from gel to the nitrocellulose membrane at 30 mA per membrane, 10 V, overnight. Transferred proteins were then stained with Ponceau S and then washed with 0.02% PBS Tween20 0.1% to remove the stain. Membranes were blocked with 5% BSA in PBS Tween20 0.1% for 45 minutes. Monoclonal mouse anti-HDAC8 (Santa Cruz Biotechnology®), diluted in 5% BSA in PBS Tween20 0.1%, was incubated overnight (4°C) with agitation, followed by three washing steps with 0.1% PBS Tween20 0.1% for 5 minutes each. Anti-mouse HRP secondary antibody (Santa Cruz Biotechnology®) at 1:25000 in 5% BSA in PBS Tween20 0.1% incubated for 1 hour at RT. Membranes were washed with PBS Tween20 0.1% (3 times) for 5 minutes each, and PBS 1X (1 time), and then proteins were probed with Clarity Max™ Western ECL Substrate (Bio-Rad). Detection was accomplished using a Fujifilm Luminescent Image Analyzer LAS-3000 v2.2 (Fujifilm, Tokyo, Japan).

2.6. Chromosome analysis

Chromosome analysis experiments were performed in peripheral blood, fibroblasts, and LCLs. Peripheral blood was cultured as described above (section 1.2). After 24 hours of initiation, cultures were treated with the following DEB (Sigma-Aldrich®) concentrations 0 µg/mL (no treatment), 0.05 µg/mL, and 0.1 µg/mL. The protocol used for this experiment was an adaptation of the protocol used in the Cytogenetics Laboratory of ICBAS for the for evaluation of chromosome instability. This protocol is already well established, and no major alterations were needed.

Fibroblast cultures were maintained under the conditions described above (section 1.2) until reaching the necessary confluence (approximately 60%). Cells were then treated with the following DEB (Sigma-Aldrich®) concentrations, 0 µg/mL (no treatment), 0.005 µg/mL and 0.01 µg/mL. Peripheral blood and fibroblast cultures were then maintained with DEB treatment for 48 hours at 37°C in a 5% CO_2 humidified atmosphere. LCLs cultures were maintained until reaching the confluence of approximately 90-95%.

After the incubation period, all cell types were treated with 100 µL of colcemid (Gibco™) for 1 hour (peripheral blood), 4 hours (fibroblasts), and 1 and half hour (LCLs) at 37°C in a 5% CO_2, humidified atmosphere. The adherent cells (fibroblasts) were then treated with 1 mL of Trypsin (Gibco™) for 5 minutes at 37ºC in a 5% CO_2, humidified atmosphere. Cells growing in suspension (peripheral blood and LCLs) and fibroblasts after trypsinization step were transferred into a 15 mL Falcon tubes and centrifuged 10 minutes at 518 g. After discarding supernatant, 9 mL of hypotonic solute (KCl) (Merck™) was added and incubated for 30 minutes at 37ºC. Cells were centrifuged 10 minutes at 518 g and fixed in an ice cold solution of methanol (Fisher Chemical™) and acetic acid (Fisher Chemical™) in a proportion of 3:1. After this step, cells were stored at 4ºC, for at least 1 and half hour. Centrifugation and fixation steps were repeated 3 times, in order to wash the cells. A small part of the resulting suspensions was then dropped onto properly labeled microscope slides, with a Pasteur pipette. Slides were left to air dry for approximately 24 hours. The maintenance of the RT (22 to 25ºC) and humidity (50 to 60%) are important factors to be considered when making the chromosome preparations since chromosomes will spread badly both in a warm and dry environment as well as in a very humid environment. Finally, the slides were stained using 3% of Giemsa (Merck™) for 4 minutes. Using the OLYMPUS CX31 microscope, chromosomes were analyzed in 100X objective.

2.7. Human androgen receptor methylation assay (HUMARA)

Three reactions were prepared, for each gDNA sample, used at final concentration of 25 ng/µL, following the methodology cited by Allen et al. (Allen et al., 1992). Two of them consist of *Rsa*I enzymatic digestion (New England BioLabs®) (frequent cutter), and the third was used as a digestion control - sample incubated with enzymatic buffer without enzyme (undigested sample). The reactions were pre-digested for 3 hours at 37°C, and then, methylation sensitive endonuclease, *Hha*I (New England BioLabs®), was added in one of the products resulting from the *Rsa*I enzymatic digestion. All reactions were incubated overnight at 37°C, followed by temperature inactivation (70°C for 20 minutes). Amplification was performed using a PCR master mix (Promega®, Madison, Wisconsin, USA) and NED labeled primers (table 11 in 1.5). Cycling conditions consisted of 5 minutes incubation at 95°C and 28 cycles of denaturation at 95°C for 45 seconds, annealing at 62°C for 30 seconds, and extension at 72°C for 30 seconds, the final extension of 15 minutes at 72°C (Figure 8). PCR products were mixed with 15 µL of formamide and 0.5 µL GeneScan™ 500 ROX™ dye Size Standard (Applied Biosystems™, Waltham, Massachusetts, USA). Fragments were separated by capillary electrophoresis on ABI PRISM® 3130xl Genetic Analyzer (Applied Biosystems™, Foster City, CA, USA) and the results analyzed using GeneMapper® Software version 4.0 (Applied Biosystems™).

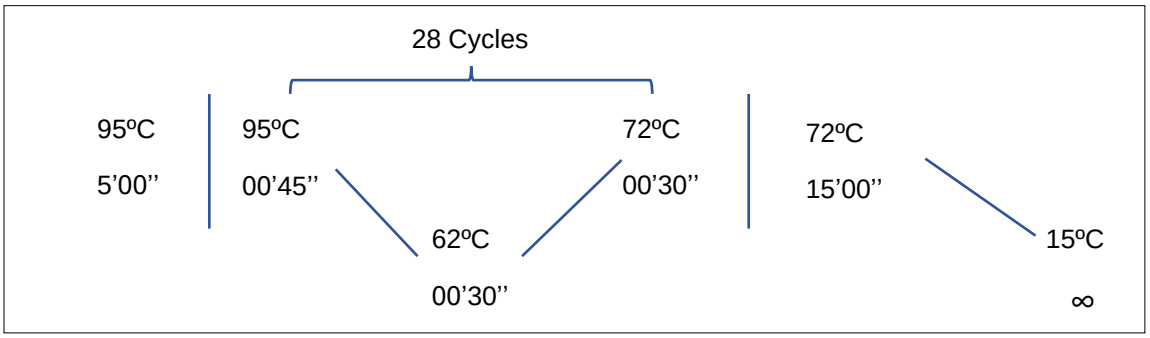

Figure 8 PCR amplification conditions.

2.8. *HDAC8* transcript analysis

RNA was obtained from the sample cell pellet used for chromosome spreads analysis, using 5 PRIME PerfectPure™ RNA Blood Kit (Thermo Fisher) (blood) and EZ1 RNA Tissue Mini Kit® (QIAGEN, Hilden, Germany) (fibroblasts and LCLs). A cDNA region harboring the exon 8 of *HDAC8* was amplified using SuperScript® One-Step - RT-PCR with Platinum® Taq kit (Invitrogen™) using the primers cDNA_*HDAC8*-F and

cDNA_*HDAC8*-R (section 1.5), following manufacturer's instructions. Amplification conditions consisted of 30 minutes at 50ºC and 2 minutes at 95°C, then 40 cycles of denaturation at 94°C for 15 seconds, annealing at 55°C for 45 seconds, and extension at 72°C for 3 minutes, the final extension of 7 minutes at 72°C (Figure 9). Symmetric PCR products were purified using the enzymatic PCR clean up technology Illustra™ ExoStar™ 1-Step (GEHealthcare Life Sciences®, Chicago, Illinois, USA). The purification was made by incubation for 30 minutes at 37ºC followed by 15 minutes at 80 ºC, which allows a quick and efficient purification of PCR products with the removal of unincorporated nucleotides and primers. The asymmetric PCR was performed using the BigDye® Terminator v3.1 cycle sequencing kit (Applied Biosystems™), according to manufacturer's instructions. The PCR conditions consisted of 1 minute incubation at 96°C and 27 cycles of denaturation at 96°C for 10 seconds, annealing at 50°C for 5 seconds, and extension at 60°C for 1 minute and 15 seconds, the final extension of 1 minute and 15 seconds at 60°C (Figure 10). After gel filtration spin columns clean up (DyeEx®96 kit, QIAGEN), products underwent capillary electrophoresis on ABI PRISM® 3130xl Genetic Analyser (Applied Biosystems™) and the results analyzed using SeqScape® Software version 2.5 (Applied Biosystems™).

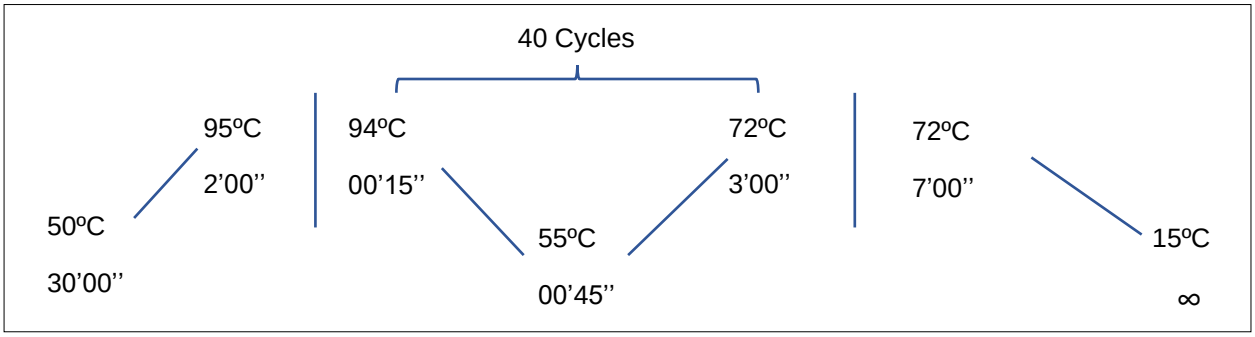

Figure 9 Symmetric PCR amplification conditions.

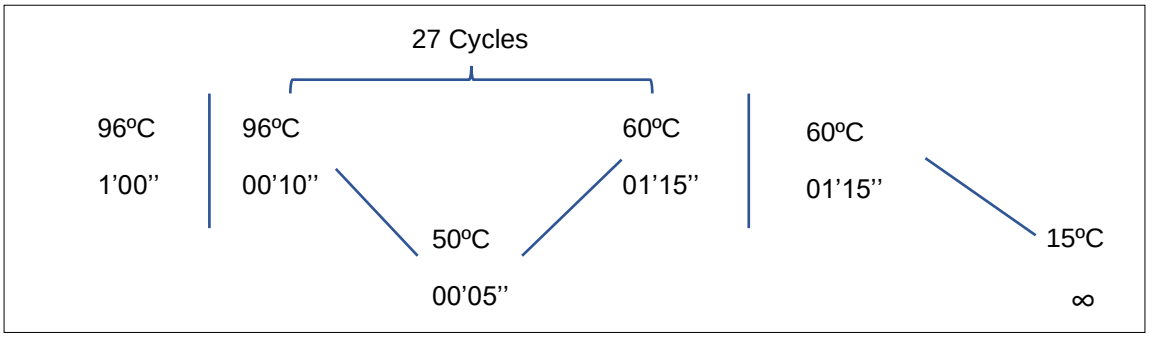

Figure 10 Asymmetric PCR amplification conditions.

2.9. Data graphing

Graphing of results obtained in immunofluorescence studies and chromosome analysis was performed using GraphPad Prism 8 Software.

RESULTS

1. HDAC8 cellular localization during mitosis

Mitotic HeLa cells were analyzed from prophase to telophase. As shown in Figure 11 to detect spindle microtubules and HDAC8 was used an tyrosinated anti-α-tubulin antibody and an anti-HDAC8 antibody, respectively. The DNA was detected using DAPI, and the chromosomes were detected using CREST antibody. It was observed that HDAC8 stained at the mitotic spindle co-localizing with tyrosinated α-tubulin at metaphase and anaphase (Figure 11A and B). Interestingly a high concentration of HDAC8 was observed in the midbody arise during telophase (Figure 11C). Further studies are needed to dissect a possible enrollment of HDAC8 in telophase and/or cytokinesis.

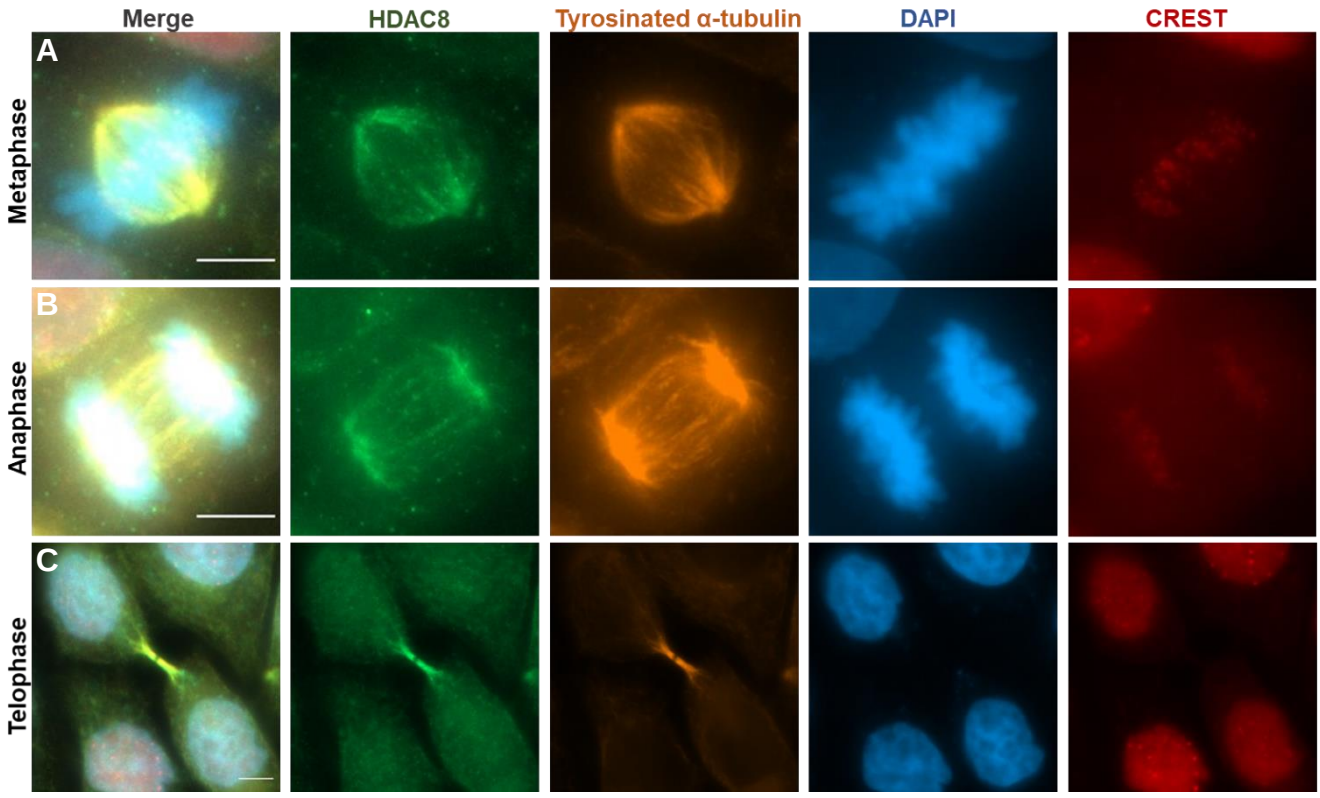

Figure 11 Immunofluorescence images of HDAC8 localization during mitosis.

HeLa cells at mitotic stages (metaphase, anaphase, and telophase) showing HDAC8 location at the spindle microtubules (A and B) and in the midbody (C). Cells were stained for HDAC8 (green), tyrosinated α-tubulin (orange), DNA (blue) and kinetochores (red). Scale bar: 10µm.

2. The role of HDAC8 in cell cycle progression

To investigate the role of HDAC8 during mitosis, loss-of-function assays using siRNA were performed in human-derived cells. As a control, a Scramble siRNA was used, targeting random sequences of RNA.

HDAC8 expression in both conditions (siScramble and si*HDAC8*) was analyzed by western blotting (WB). However, WB analysis revealed an unspecific signal for the HDAC8 antibody (Figure 12). Although WB analysis revealed a decreased overall signal in the depleted conditions further optimization, such as the inclusion of a positive control, increase the protein loaded concentration and the primary antibody dilution, change lysis and blocking buffers, are needed.

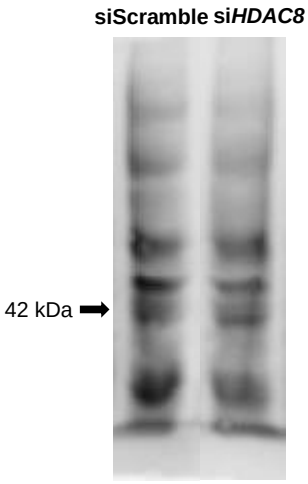

Figure 12 Western blotting analysis of control (siScramble) and HDAC8-depleted cells (si*HDAC8*)

A decrease in multiples bands along the lanes was observed in the depleted conditions. This result might reflect the HDAC8 antibody unspecificity and/or the need to further optimize the conditions used. Black arrow represents the HDAC8 band.

To confirm the success of si*HDAC8* depletion HDAC8 expression by immunofluorescence studies were analyzed (Figure 13). The HDAC8 signal in *HDAC8* siRNA condition was lower when compared to Scramble siRNA, in different mitotic phases, e.g. metaphase and anaphase.

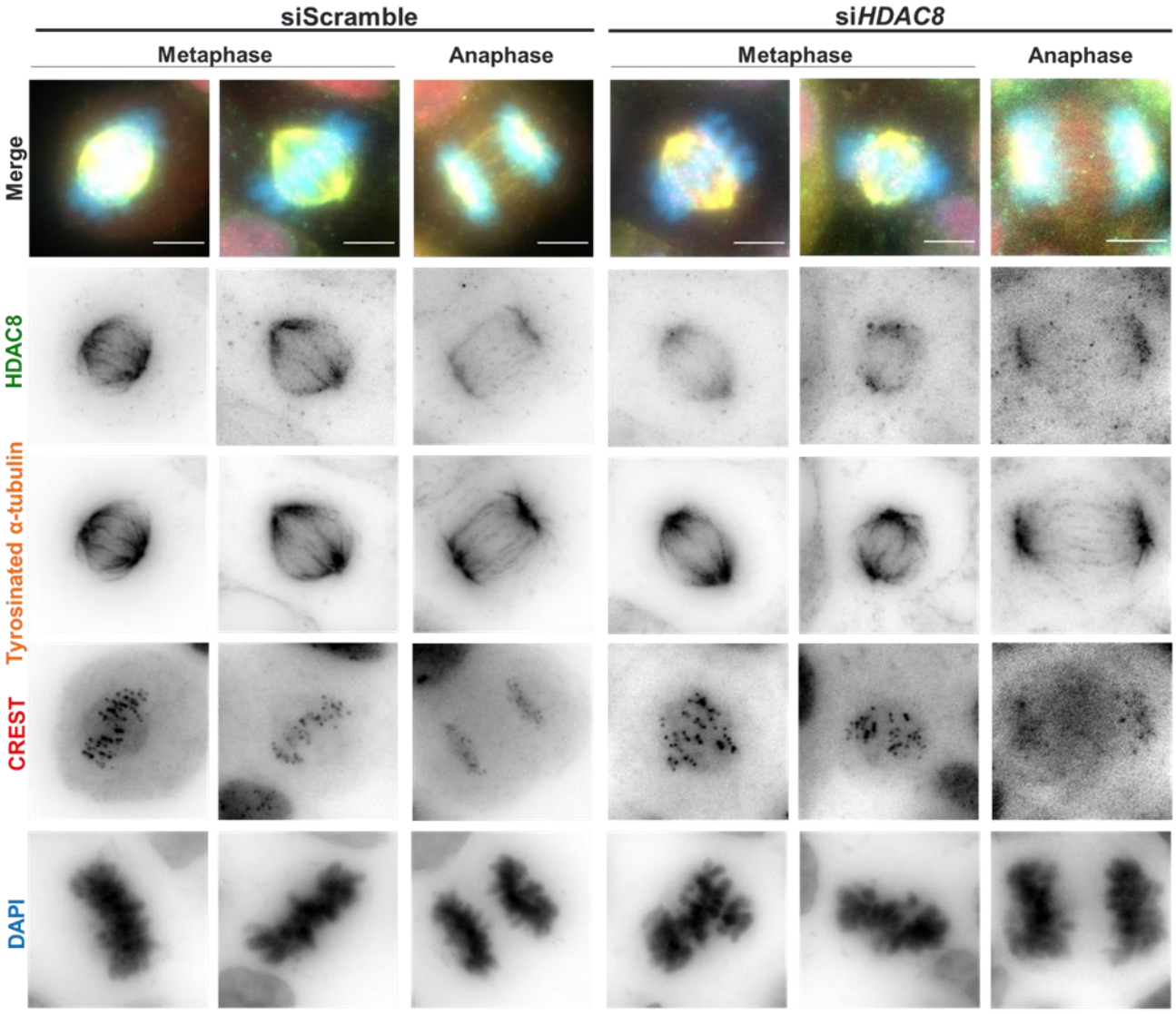

Figure 13 HeLa cells immunofluorescence studies after depletion treatments.

HDAC8-depleted and control HeLa cells during metaphase and anaphase stages. Cells treated with siHDAC8 show a decrease in HDAC8 signal when compared with cells treated with siScramble. HDAC8 was immunostained with anti-HDAC8 antibody, α-tubulin with tyrosinated α-tubulin antibody, kinetochores with CREST and DNA with DAPI. Scale bar: 10µm.

Interestingly, in HDAC8-depleted cells chromosomes were not correctly aligned at the metaphase plate, as shown in Figure 13 (si*HDAC8* condition metaphase cells). These observations are in agreement with those published by Zhang et al., prompting mitotic fidelity studies.

After confirming the HDAC8 depletion our next step was to analyze the mitotic fidelity. It should be noted that the cell line chosen for this project is a cancer cell line that usually shows some mitotic errors when compared to other types of cells such as primary cells. In an attempt to avoid bias, a comparison with the correspondent control condition in the same cell line was performed in all experiments.

Chromosome misalignment was observed at the metaphase plate in HDAC8-depleted cells (Figure 13, on the metaphase cells of si*HDAC8* condition). This leads to speculate that errors in spindle assembly and kinetochore attachments are frequently observed in depleted cells. As such errors might compromise mitotic fidelity, next were performed immunostaining analysis using fixed cells in HDAC8-depleted and control siScramble transfected cells.

Seventy-two hours after transfection, si*HDAC8* and control siScramble HeLa cells were fixed and immunostained with DAPI. In order to describe the mitotic index and profile, 800 control condition (siScramble) cells and 800 HDAC8-depleted cells were observed in interphase and mitotic phases (prophase, prometaphase, metaphase, anaphase, and telophase). A similar number of cells were obtained in siScramble: 35 mitotic cells (4.375%) and HDAC8-depleted cells: 37 mitotic cells (4.625%), indicating that depletion does not affect their mitotic index (Figure 14A). Notably, a lower cell growth in HDAC8-depleted condition was observed when compared to control. Focusing on the mitotic population, HDAC8-depleted cells presented a pronounced decrease of cells in prophase or prometaphase (22%) when compared to siScramble (48%) (Figure 14B). That observation led to the speculation that those cells might not be controlling errors in prophase/prometaphase in accordance with a defective metaphase plate. Similarly, in si*HDAC8* cells the values of metaphase (35%), anaphase (24%), and telophase (19%) were higher than in Scramble siRNA (23%, 14%, and 14%, respectively) (Figure 14B).

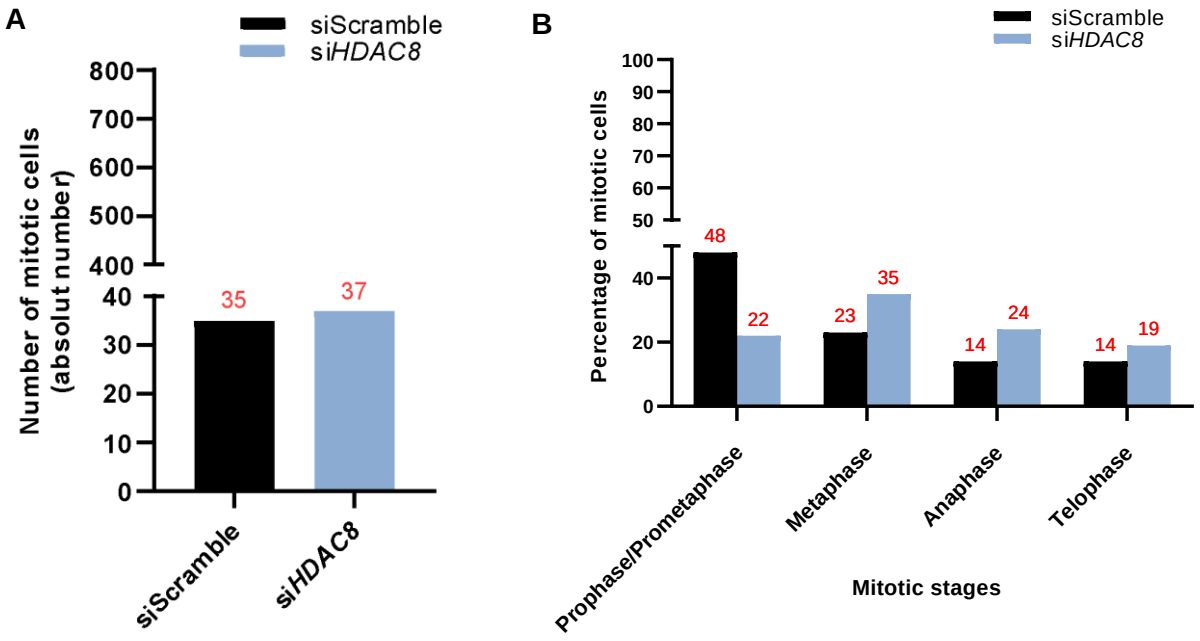

Figure 14 Quantification of mitotic cells after transfection experiments.

A) Number of mitotic cells siScramble (control, 35) and si*HDAC8* (37) a total of 800 cells.
B) Percentage of mitotic cells in different mitotic stages: prophase/prometaphase, metaphase, anaphase, and telophase in siScramble and in si*HDAC8* depletion conditions.

Interestingly, a higher percentage of chromosome misalignment in HDAC8-depleted HeLa cells was noticed when compared to the control. This can be explained by defects in KT-MTs attachments. More studies are thus needed to prove this hypothesis and dissect the role of HDAC8 in KT-MTs attachments.

As shown in Figure 15A, in si*HDAC8* condition different types of errors was observed during mitosis such as chromosome congression failure (Figure 15A, I), multipolar cells (Figure 15A, II), lagging chromosomes (Figure 15A, III) and chromatin bridges (Figure 15A, IV).

The ratio of lagging chromosomes in anaphase cells increased from 3% in the siScramble to 12% in HDAC8-depleted cells. Concomitant to this, the chromatin bridges that remain in telophase increased from 0% to 6 % of total telophase cells. Chromosome congression during prometaphase also increased from 0% to 8%. Interestingly, multipolar mitotic spindles not detected in siScramble were present in 6% of mitotic HDAC8-depleted cells (Figure 15B).

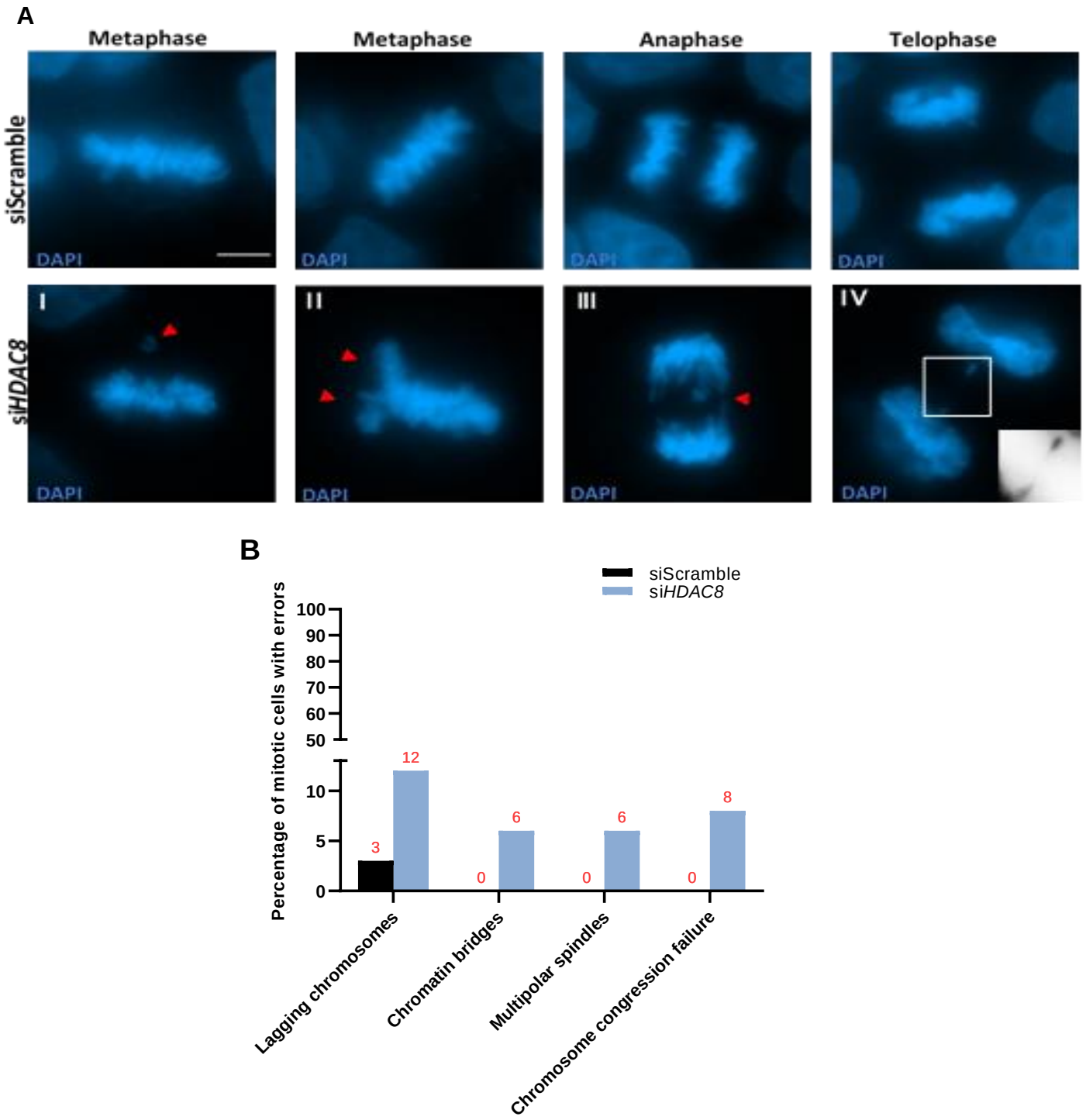

Figure 15 Mitotic errors in siScramble and si*HDAC8* transfected HeLa cells.

A) Examples of errors during different stages of mitosis (metaphase, anaphase and telophase). Correct segregation of DNA during mitosis of control cells (siScramble). Cells after si*HDAC8* treatment showing several mitotic defects (red arrows): I- chromosome congression failure; II- Multipolar spindle (tripolar cell); III- Lagging chromosome; IV- Chromatin bridge. DAPI was used to stain DNA. Scale bar: 10µm.

B) Percentage of lagging chromosomes, chromatin bridges, multipolar spindles, and chromosome congression failure in siScramble and si*HDAC8* cells.

Several immunofluorescence images of HDAC8-depleted cells with defects and tyrosinated α-tubulin simultaneously stained were included in order to clarify the drastic phenotype and presence of errors in different mitotic stages (Figure 16).

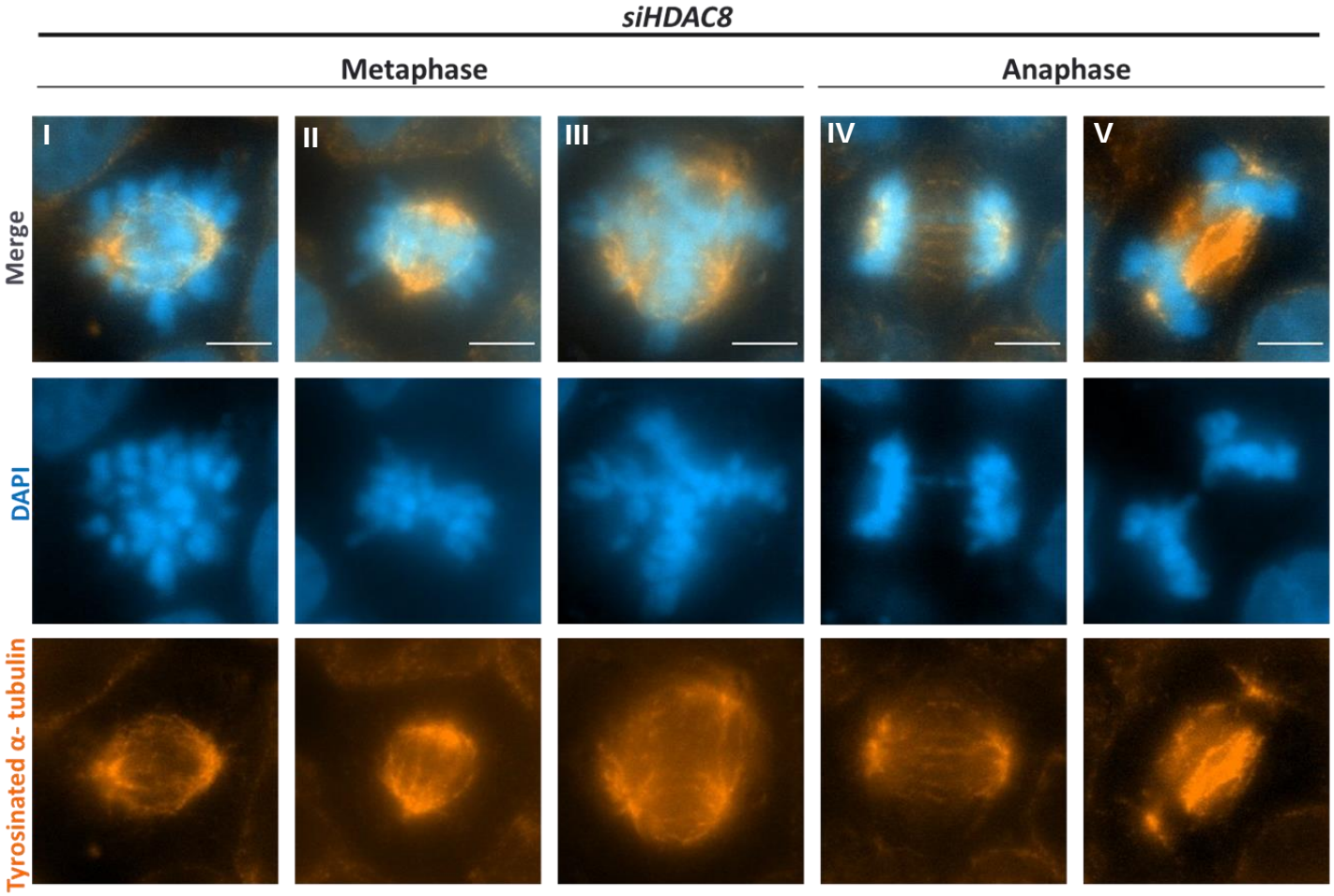

Figure 16 Mitotic errors in HDAC8-depleted cells.

Examples of errors observed in metaphase, anaphase, and telophase: I and II- Chromosome congression failure; III- Multipolar spindle (quadripolar cell); IV and V- Chromatin bridges. DAPI was used to stain DNA (blue) and tyrosinated α-tubulin antibody to stain α-tubulin (orange). Scale bar: 10 µm.

3. Impact of a mutant *HDAC8* allele in chromosome instability and its expression

3.1. Experimental planning

To further understand the implications of HDAC8 in the maintenance of ploidy, primary cells from a female affected individual presenting a heterozygous *HDAC8* variant were used. The missense variant c.793C>T; p.(Gly265Arg) is described as likely pathogenic at ClinVar (RCV000680270.1) and dbSNP (rs1569318004) databases, but without frequency information (Yuan et al. 2019). Overall bioinformatics analysis suggests a plausible candidate causative variant. Additionally, the cells were challenged with the DNA damage agent 1,3-Butadiene diepoxide (DEB), as HDAC8 has been associated with DNA damage response pathway, ensuring DNA integrity. When cells are sensitive to DEB mechanisms of DNA repair are compromised leading to DNA damage aberrations, such as chromosome breaks (Figure 17A), fragments (Figure 17B), and/or radial figures (Figure 17C). Chromosome instability was evaluated using the parameter percentage of aberrant cells.

The gold-standard experiment to study cell's ploidy is to prepare chromosome spreads from fresh samples. A normal karyotype presents 46 chromosomes (Figure 17D), whereas aneuploid cells have more chromosomes (hyperdiploid) (Figure 25A) or less (hypodiploid) (Figure 17C).

To clarify if cells from this affected individual also show aneuploidies and/or chromosome instability, peripheral blood, fibroblasts, and Epstein-Barr virus (EBV) transformed human B lymphocytes; or human B lymphoblastoid cells (LCLs) were analyzed**.** Additionally, peripheral blood samples from its parents and a healthy donor (control) were also analyzed.

X chromosome inactivation (XCI) is an important gene regulation mechanism in females to equalize the expression levels of the X chromosome between the two sexes. In most cases, one of the two X chromosomes in females is randomly chosen to be inactivated (Wang et al. 2019). Expression of mutant alleles in heterozygous females has been ascribed to skewed X-chromosome inactivation, which has been reported to play an important role in many X-linked diseases (Busque et al. 1994).

The human androgen receptor methylation (*AR*) gene (HUMARA) assay was used to determine the XCI pattern in proband and its parents. However, the proband's sample was found to be uninformative for the *AR* CAG repeat polymorphism, which hampered further XCI analysis. Therefore, *HDAC8* transcript analysis were performed in order to analyze the RNA expression of *HDAC8.*

The following results are divided by sample origin due to their differential HDAC8 expression and sensitivity to the agents used in each experiment.

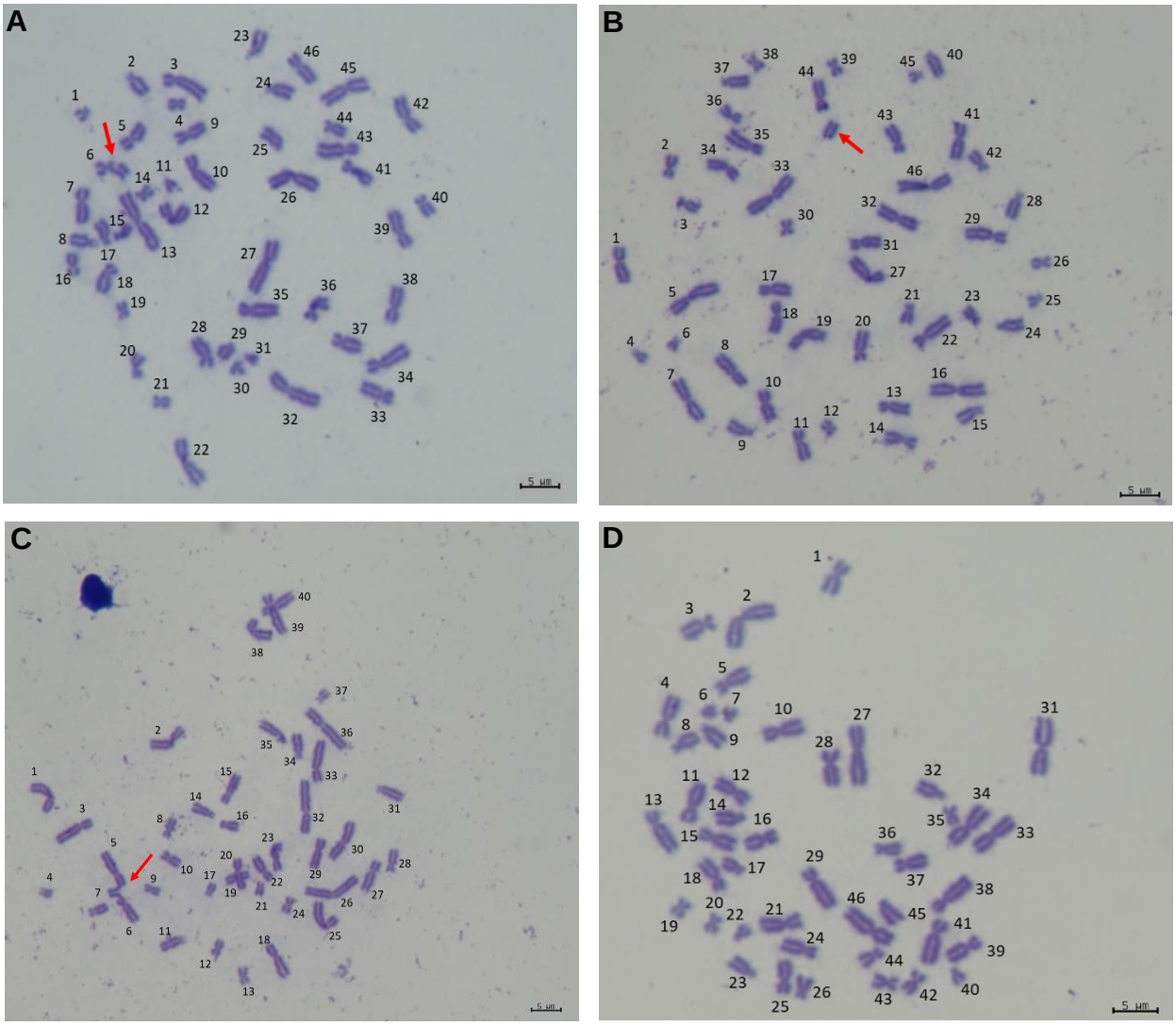

Figure 17 Karyotype analysis of the peripheral blood from the affected individual, showing different types of aberrations.

A) Normal ploidy (46 chromosomes) with a chromosome break (red arrow).

B) Normal ploidy (46 chromosomes) with a chromosome fragment (red arrow).

C) Aneuploidy (40 chromosomes) and a radial figure (red arrow).

D) Cell with normal ploidy (46 chromosomes).

All cells were analyzed using a 100x objective magnification. Scale bar: 5µm.

3.2. Peripheral blood analysis

3.2.1. Chromosome instability and ploidy analysis

In order to investigate the patterns of spontaneous and induced chromosome instability in peripheral blood samples from proband and parents, cells were treated with different DEB concentrations (0.00 µg/mL of DEB in spontaneous condition and 0.005 µg/mL or 0.01 µg/mL in DEB treated conditions). The used methodology is described in section 2.6.

As shown in Figure 18, in spontaneous conditions, was not observed a significant difference in the percentage of aberrant cells between healthy donors, from now named as control, (0%), the proband (2%), father (0%), and mother (1%) (Figure 18).

With low doses of DEB, 0.05 µg/mL, the percentage of aberrant cells was also similar between the control (5%) and the proband (8%), father (4%), and mother (6%).

A significant increase in the number of aberrant cells (with chromosome breaks, fragments, and/or radial figures) was observed in the proband (51%) when compared with the control (10%), father (11%) mother (17%), using the higher doses of DEB (Figure 18).

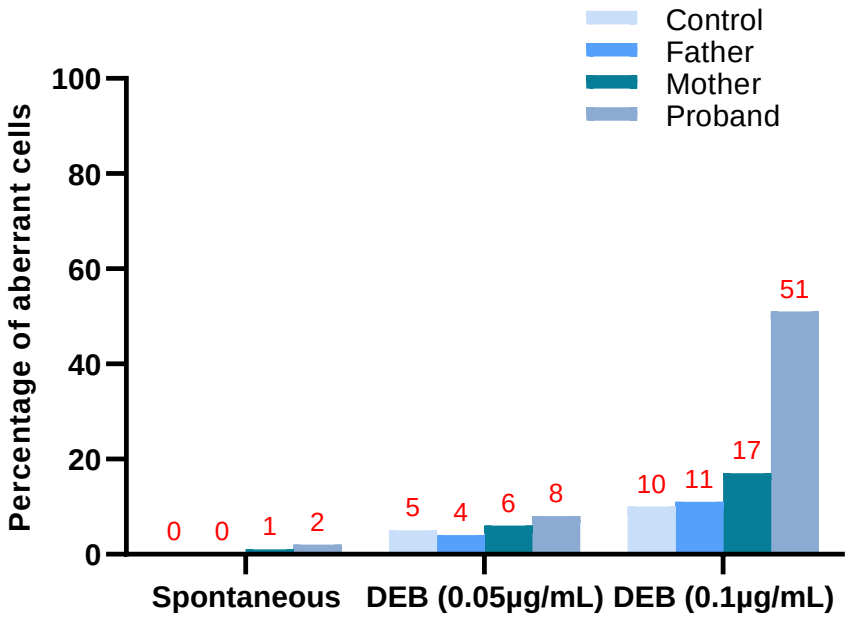

Figure 18 Percentage of DEB-induced aberrant cells analysis in peripheral blood cells.

Percentage of aberrant cells in cells without treatment (spontaneous conditions) and treated with DEB 0.05 or 0.1 µg/mL. A significant increase of DEB (0.1 µg/mL) induced aberrant cells was observed in the proband when compared with control, father, and mother samples.

Cell ploidy was analyzed without DEB addition to mimic the *in vivo* condition. The total number of chromosomes in each cell from control, father, mother and proband samples were scored in a total of 100 chromosome spreads (Figure 19).

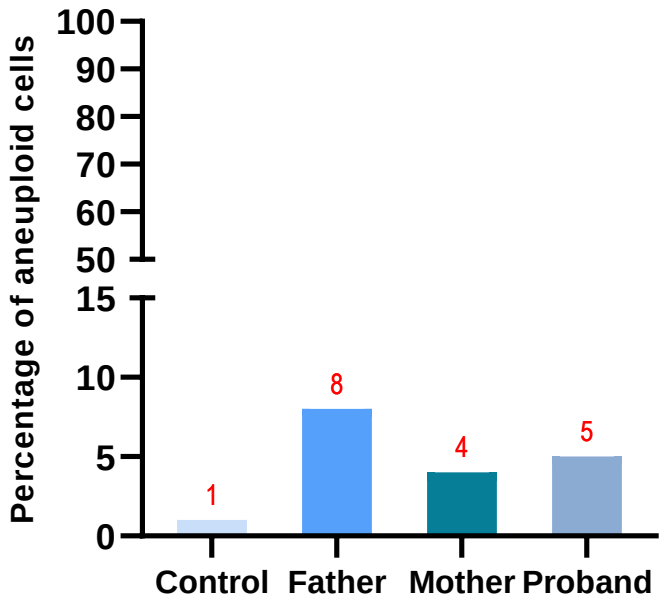

Figure 19 Ploidy analysis in peripheral blood cells.

Percentage of aneuploidy observed in control, father, mother and proband cells. No significant alterations were observed.

3.2.2. *HDAC8* mutant allele expression studies

As shown in Figure 20, the human androgen receptor methylation (*AR*) gene (HUMARA) assay revealed an uninformative result for the *AR* CAG repeat polymorphism in proband's sample.

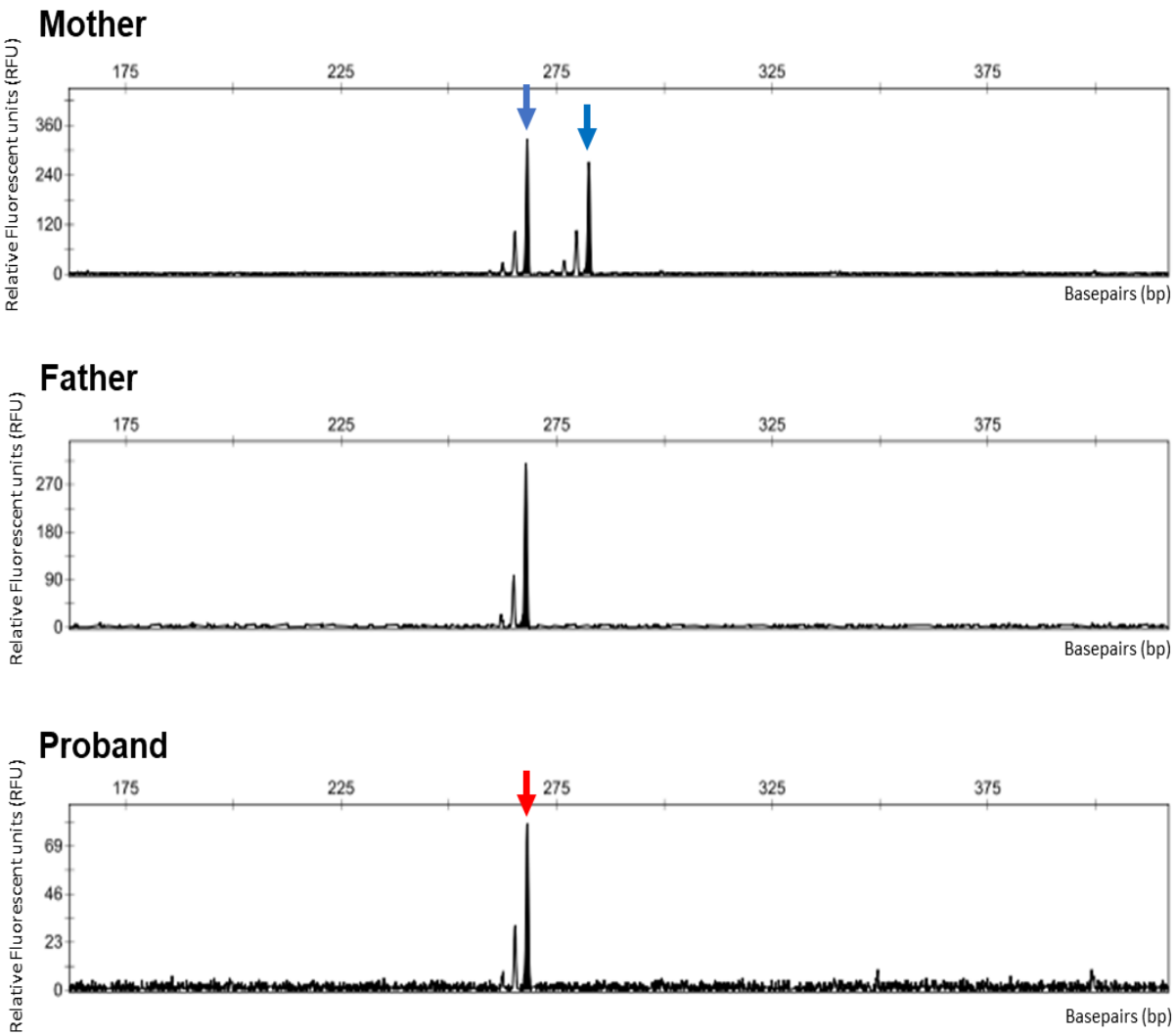

Figure 20 *AR* gene CAG repeat polymorphism analysis.

Mother showed two alleles with distinct sizes. Proband's sample revealed to be uninformative as an allele with same size was both maternally and paternally inherited (homoallelic, red arrows).

To investigate the RNA expression profile of *HDAC8* alleles, *HDAC8* RNA expression analysis of the *HDAC8* transcripts were performed following the methodology described in section 2.8, albeit the technical biases and limitations of cDNA sequencing methodological approach. The RNA expression profile analysis showed that only the normal *HDAC8* allele is expressed in peripheral blood (Figure 21, red arrow). The apparent unique expression of the normal allele in this tissue can be due to the complete inactivation of the mutant allele (in case of an X-chromosome inactivation skewed pattern), or to an amplification bias, or due to a limited ability to accurately quantify lowly expressed alleles.

Consequently, these results do not allow a direct correlation between the presence of aberrant cells, observed using DEB 0.1 µg/mL and the expression of the mutant *HDAC8* allele in peripheral blood.

To further understand the involvement of HDAC8 in the maintenance of ploidy and chromosome instability the same experiments were next reproduced in cultured fibroblasts.

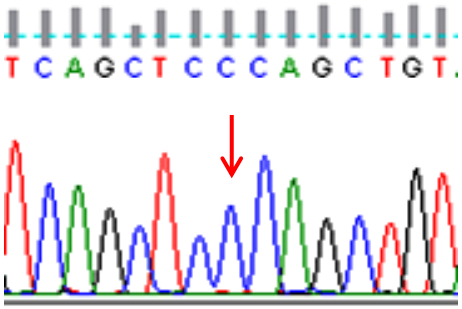

Figure 21 Partial electropherogram of *HDAC8* (exon 8) cDNA sequencing.

HDAC8 RNA expression profile in peripheral blood. Red arrow indicates the position where the DNA mutation occurs. Only the normal “C” nucleotide is observed.

3.3. Cultured fibroblasts analysis

3.3.1. Chromosome instability and ploidy analysis

To investigate genomic instability in cultured fibroblasts, proband and control cells were treated with different concentrations of DEB (0.00 µg/mL of DEB in spontaneous condition and 0.05 µg/mL or 0.1 µg/mL of DEB in DEB treated conditions) as described in section 2.6.

Chromosome spreads in DEB treated conditions did not reveal any significant difference in the percentage of aberrant cells in control (0% in spontaneous conditions, 2% in DEB 0.005 µg/mL and 5% in DEB 0.01 µg/mL) and proband samples (0% in spontaneous conditions, 8% in DEB 0.005 µg/mL and 13% in DEB 0.01 µg/mL) (Figure 22).

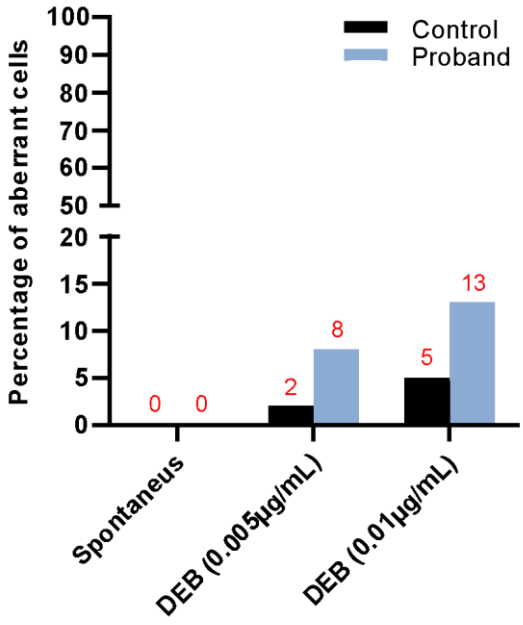

Figure 22 Percentage of aberrant cells in cultured fibroblasts.

Percentage of aberrant cells in different DEB concentrations in control and proband. No significant difference was detected in proband compared with control.

The analysis of the cell's ploidy revealed a significant increase in the percentage of aneuploid cells in proband (30%) when compared to the control (7%) (Figure 23). *HDAC8* expression profile in cultured fibroblasts was then analyzed.

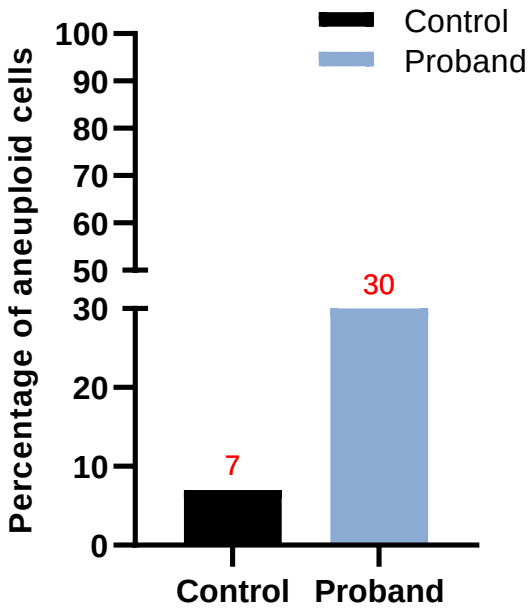

Figure 23 Ploidy analysis of cultured fibroblasts.

Percentage of aneuploid fibroblasts cells in control and proband fibroblasts. An increased number of aneuploid cells was observed in proband when compared with control cells.

3.3.2. *HDAC8* mutant allele expression studies

The analysis of *HDAC8* expression profiles followed the same methods previously used in peripheral blood. A small signal corresponding to the *HDAC8* mutant allele "T" was observed suggesting that this allele seems to be expressed in fibroblasts (Figure 24, red peak in red arrow position). This result can be explained by an amplification bias, a limited ability to quantify lowly expressed alleles, or somatic mosaicism. Overall the results obtained in fibroblasts do not allow a direct correlation of the mutant *HDAC8* allele and the presence of in this cell type.

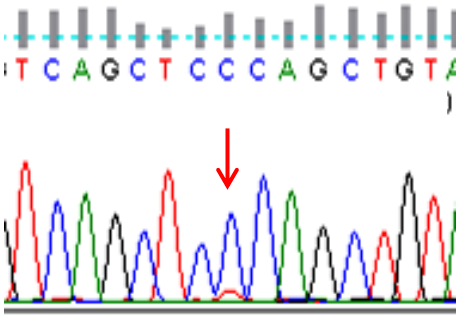

Figure 24 Partial electropherogram of *HDAC8* (exon 8) cDNA sequencing.

HDAC8 RNA expression profile of the two alleles. Red arrow indicates the expression of both nucleotides: "C" (normal) and "T" (mutated).

3.4. LCLs analysis

3.4.1. Ploidy analysis

The analysis of the 100 chromosome spreads, following the methodology described in section 2.6, revealed a surprisingly high percentage of aneuploidies. Seventy-six per cent of the cells showed aneuploidies with extra (Figure 25A) or missing chromosomes (Figure 25B), and only twenty-four per cent of the cells had normal number of chromosomes (46 chromosomes).

RNA expression studies using the same methods previously described for peripheral blood and fibroblasts were also performed.

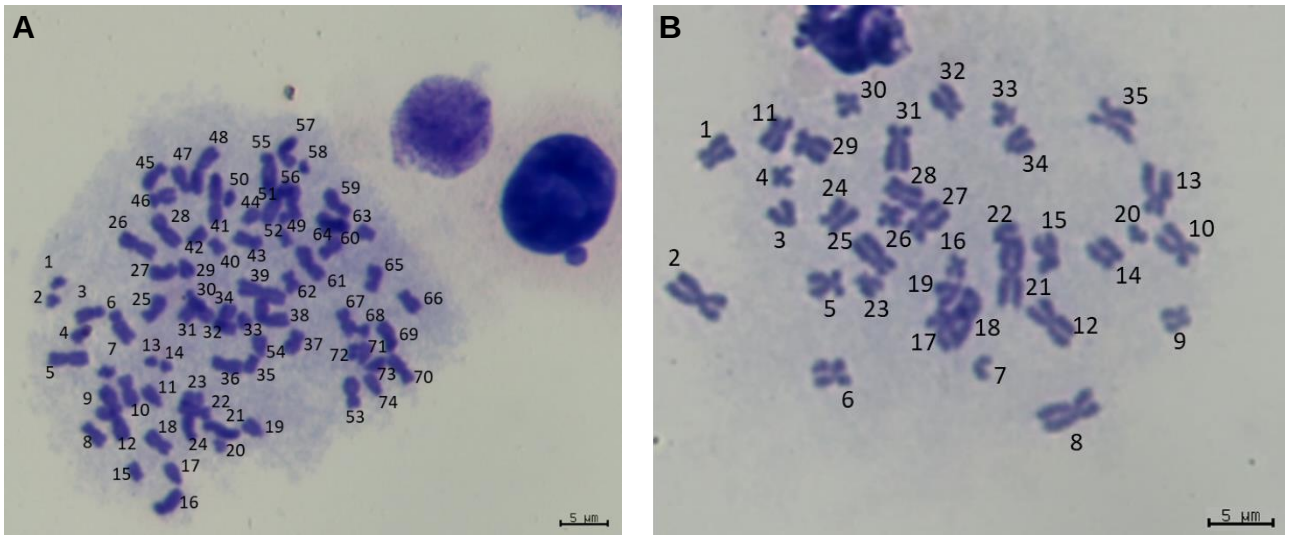

Figure 25 Karyotype analysis of the lymphoblastoid cells.

A) Aneuploid cell with 74 chromosomes (hyperdiploid).

B) Aneuploid cell with 35 chromosomes (hypodiploid).

All cells were analyzed using a 100x objective magnification. Scale bar: 5µm.

3.4.2. *HDAC8* mutant allele expression studies

The analysis of *HDAC8* expression profiles of the *HDAC8*, following the same methods previously used in peripheral blood and cultured fibroblasts, revealed that the *HDAC8* mutant allele, “T” is also expressed in LCLs (Figure 26, red peak in red arrow position). This result can be explained by an amplification bias, a limited ability to quantify lowly expressed alleles, or somatic mosaicism. Overall the results obtained in fibroblasts and LCLs seem to suggest a correlation between the mutant HDAC8 allele and the presence of aneuploidy in those cell types.

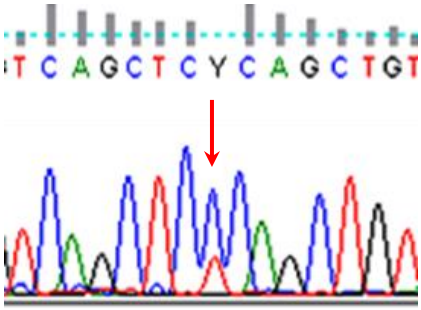

Figure 26 Partial electropherogram of *HDAC8* (exon 8) cDNA sequencing.

HDAC8 RNA expression profile. Red arrow indicates the expression of both nucleotide: “C” (normal) and “T” (mutated).

DISCUSSION

In recently years, the precise localization and role of some class I HDACs during cell cycle progression has been widely explored. This understanding is of utmost importance to dissect the mechanisms involved in the maintenance of mitotic fidelity.

In this project, we aimed to uncover the HDAC8 location during cell cycle progression (prophase/prometaphase, metaphase, anaphase, and telophase), the role in mitotic fidelity and consequently in the maintenance of cell's ploidy. This work represents a unique opportunity to dissect, for the first time, the role of HDAC8 in the accuracy of mitosis using HeLa cells and human-derived cells from an affected individual with an *HDAC8* variant.

1. HDAC8 localization during mitosis

The HDAC8 was previously reported as a tubulin deacetylase, more specifically as a deacetylase of the acetylated α-tubulin, which is considered as a marker of microtubules stabilization (Vanaja, Ramulu, and Kalle, 2018). Our studies showed HDAC8 location at the mitotic spindle during metaphase and anaphase and in the midbody during telophase. These results are consistent with a previous report in mouse oocytes where HDAC8 was shown to be concentrated on the spindle poles to co-localize with γ-tubulin during meiotic maturation (Zhang et al., 2017). These authors suggested, for the first time, the involvement of HDAC8 in spindle organization. Interestingly, the co-localization with tyrosinated α-tubulin was also observed in HeLa cells. Our observations allow us to speculate that HDAC8 might have a function in spindle microtubule organization and consequently in the mitotic fidelity ensuring. It is important to underline that these findings were observed for the first time in human cells. The presence of HDAC8 in the midbody led us to hypothesize a possible enrollment of HDAC8 in telophase and/or cytokinesis, to be explored in future works.

2. The role of HDAC8 in cell cycle progression

To highlight the role of HDAC8 in cell cycle progression knockdown studies were conducted. The success of HDAC8 depletion was confirmed only by immunofluorescence studies, as the western blotting analysis needs to be further optimized to obtain a specific signal.

In our experiments, the mitotic index was not affected in HDAC8-depleted cells. Nevertheless, we observed lower cell growth in HDAC8-depleted condition compared with control, which can be caused by a decreased number of cells that were entering mitosis. In fact, HDACs have been implicated in regulating cell migration and progression; low levels of mitotic cells in comparison with levels of interphasic cells (G0, G1 and S) in HDAC8-depleted cells have also been reported. This is in line with the role of HDAC8 in HeLa as predominant deacetylase of α-tubulin, which in turn is involved in regulating cell cycle in the G2/M phase (Vanaja, Ramulu, and Kalle, 2018). Additionally, HDAC8 inhibition led to a delay in cell cycle progression, suppression of proliferation, and induced apoptosis (Dasgupta et al., 2016). In mitotic HeLa cells, we observed a significant decrease of prophase/prometaphase cells in HDAC8-depleted cells when compared with control. These results led us to speculate that cells are not controlling errors in prophase/prometaphase in accordance with a defective metaphase plate. In, the other mitotic phases (such as metaphase, anaphase, and telophase) an increased number of cells in HDAC8-depleted population was observed which led us to believe that the mitotic cells exit occurs more slowly when HDAC8 was not present. Further studies are needed to better understand the effects of the HDAC8-depletion in migration and cell cycle progression in HeLa cells.

Another goal of our project was to dissect the HDAC8 involvement in mitotic fidelity and consequently the occurrence of segregation errors when deregulated. To achieve this, the frequency of cells with errors in HDAC8-depleted population was determined. Errors such as chromosome congression failure in metaphase, multipolar mitotic spindles and lagging chromosome in anaphase, and chromatid bridges in telophase were detected in higher frequency in HDAC8-depleted cells compared to the control. These findings corroborate with previous studies where HDAC8 was proposed to participate in proper spindle assembly and chromosome alignment, protecting mouse eggs from aneuploidy (Zhang et al., 2017).

HDAC8 is required for proper spindle organization and kinetochore-microtubule attachments to maintain ploidy in mouse. In future experiments, we plan to measure the spindle length and morphology as they depend on the regulation of microtubule dynamics during spindle formation and the establishment of the kinetochore-microtubule attachments. Another important consideration is the correct kinetochore-microtubule attachments known to be required for correct chromosome segregation. Overall unraveling these mechanisms will highlight the role of HDAC8 in mitotic fidelity implicated in the generation of aneuploidy.

3. Impact of a mutant *HDAC8* allele in chromosome instability and its expression

Errors during cell division, including the unbalanced allocation of chromosomes, can lead to aneuploidy (Han et al., 2015; Zhang et al., 2017). Moreover, it is widely accepted that an extra or missing chromosome is an important cause of genetic disorders as well as birth defects and cancer (Sen, 2000). Previous findings showed that HDAC8 localizes at spindle poles to participate in proper spindle assembly and chromosome alignment, protecting mouse eggs from aneuploidy. In line with our observations in HeLa cells, we speculate that HDAC8 can be involved in ensuring the cell's ploidy through the maintenance of mitotic fidelity.

The HDAC8-dependent cohesin complex is well known to accumulate at DNA break sites to mediate DNA repair and recruit cell cycle checkpoint-activating proteins (Watrin and Peters, 2009). Moreover, HDAC8 has been involved in DNA repair pathways once its inhibition led to an increase of DNA damage in Multiple Myeloma when cells are exposed to radiation. HDAC8 is recruited to double strand break sites to repair this DNA damage, suggesting a novel function of HDAC8 in promoting DNA repair pathways in Multiple Myeloma cells (Chyra et al., 2019). That evidence led us to hypothesize that HDAC8 can have a role in the DNA damage response pathway, ensuring DNA integrity.

To further validate our hypothesis, we used different DEB -a DNA damage agent- treated cell lines from an affected individual (proband) with a heterozygous *HDAC8* missense variant.

Proband peripheral blood sample revealed a higher percentage of aberrant cells, but not aneuploidies, after DEB 0.1 µg/mL treatment when compared with control and parents (father and mother). In contrast with other cell types –see below- the peripheral blood only expressed the normal *HDAC8* allele, observed after cDNA sequencing in the proband, hampering the implication of this HDAC8 missense variant in the cell's phenotype.

In contrary to the peripheral blood, proband's cultured fibroblast revealed a significant increase of aneuploid cells concomitant to the expression of the mutant allele after cDNA analysis. Although the involvement of other genes/proteins cannot be excluded, the expression of this HDAC8 variant may explain the aneuploidies and led us to speculate that HDAC8 plays a significant role in ensuring the ploidy of cells, corroborating our previous HeLa cells. To further support our hypothesis proband's EBV-transformed lymphocytes cells were generated and investigated, revealing a similar result to that obtained in fibroblasts, either in terms of aneuploidy number and mutant allele

expression. Although we observed a small increase in aberrant cells in all proband's samples when compared to the control, the involvement of this mutant *HDAC8* in DEB induced DNA damage cells in proband's samples seems unlikely.

In order to that, the *HDAC8* mutant allele can be the cause of the high percentage of aneuploid cells found in fibroblasts we analyzed LCLs from the proband carrier of the *HDAC8* mutant allele. The analysis of chromosome spreads showed a considerably high number of aneuploid cells. Importantly, the *HDAC8* expression profile revealed that mutant allele is expressed, and its expression is higher than in fibroblast. That is in line with a higher percentage of aneuploid cells found in LCLs compared with fibroblasts. Such findings support our hypothesis that HDAC8 protein plays a crucial role in the ensure of the cell's ploidy since the expression of the missense mutant *HDAC8* allele can be directly correlated with the increase of aneuploid cells.

The implication of HDAC8 in mitotic fidelity to ensure a correct chromosome segregation and consequently maintain cell ploidy has paved the way to the understanding of HDAC8 implication in diseases such as Cornelia de Lange Syndrome and cancer.

CONCLUSIONS

The present project represents an important step to unravel HDAC8 function in mitosis, allowing for the first time the following key findings:

1. HDAC8 location at the mitotic spindle co-localizing with tyrosinated α-tubulin at metaphase and anaphase, and in the midbody at telophase during mitosis in HeLa cells.
2. Observation of high number of lagging chromosomes, chromatin bridges, chromosome congression failure, and multipolar mitotic spindles, in HeLa HDAC8 depleted cells.
3. Implication of HDAC8 in aneuploidy, in established human cell line.

In line with previous studies in mice, these observations suggest that HDAC8 plays an essential role in preserving mitotic fidelity and ploidy safeguard, contributing to a better understanding of the pathophysiological mechanisms underlying not only a rare genetic syndrome but also cancer, as HDAC8 is considered a key “epigenetic player” implicated in deregulated expression or interaction with transcription factors critical to tumorigenesis.

FUTURE PERSPECTIVES

These studies were implemented, for the first time, in human-derived cell lines for the first time. Despite these major advances, some questions remain to be answered. We propose to clarify the role of HDAC8 in aneuploidy and the molecular pathways involved in the regulation of mitosis fidelity, and consequently in tumorigenesis.

We aim to perform live cell experiments to have a more consistent idea of the mitotic duration, explore the co-localization and interaction with other proteins important to ensuring the mitotic fidelity such as γ-tubulin and analyze interphasic and mitotic cells to infer about the implications of HDAC8-depletion in cell migration and progression.

Increase the statistical power of our results particularly on the number of abnormalities observed during mitosis. To this purpose, we aim to reproduce our previous experiments in more detail and search for other abnormalities in both HeLa cells and affected individual samples. This can give us further insights on the HDAC8 implication in mitotic fidelity.

Analyze the Kinetochore-MT attachments in HDAC8-depleted conditions, since it was previously reported that in mouse oocytes, HDAC8 is required for the correct Kinetochore-MT attachments. Furthermore, we also want to test the possibility of a defective spindle. For that, we will test the instability of the spindle microtubules in response to “cold treatment” as it is known that spindle microtubules without stable kinetochore attachment are unstable and are selectively destroyed by cold temperatures.

Using our CdLS-HDAC8 yet unpublished case as a model, we propose implementing a new experimental strategy for efficient functional testing of novel intellectual disability candidate variants, overcoming this bottleneck in translational medical research. Real Time-Polymerase Chain Reaction (RT-PCR) using a TaqMan probe will be used to quantify the expression of mutant HDAC8 allele, in all cell types belonging to our affected individual.

We will perform directed mutagenesis studies, to introduce our proband’s specific point mutation as well as other *HDAC8* variants publicly available (e.g. ClinVar) to have clues on the consequences of those mutations. We anticipate that understanding the causal molecular mechanisms leading to CdLS–HDAC8 will provide insights into basic processes underlying other disorders related not only to brain development but also with cancer epigenetics. In addition, the accurate identification of novel disease-associated genes/variants will enable early disease biomarkers, detailed genotype-phenotype correlation leading to precise genetic testing and counseling and, likely, the development of personalized therapeutic approaches.

BIBLIOGRAPHY

Alam N., Zimmerman L., Wolfson N.A., Joseph C. G., Fierke C.A, and Schueler-Furman O., 2016. Structure-Based Identification of HDAC8 Non-Histone Substrates. *Structure.* 24(3): 1–23.

Allen R.C., Zoghbi H.Y., Moseley A. B., Rosenblatt H. M., and Belmont J. W., 1992. Methylation of HpaII and HhaI Sites near the Polymorphic CAG Repeat in the Human Androgen-Receptor Gene Correlates with X Chromosome Inactivation. *American Journal of Human Genetics.* 51(6): 1229–39.

Amin Sk A., Adhikari N., and Jha T., 2017. Structure-Activity Relationships of Hydroxamate-Based Histone Deacetylase-8 Inhibitors: Reality behind Anticancer Drug Discovery. *Future Medicinal Chemistry.* 9(18): 2211–37.

Amin Sk A., Adhikari N., and Jha T., 2018. Diverse Classes of HDAC8 Inhibitors:In Search of Molecular Fingerprints That Regulate Activity. *Future Medicinal Chemistry.* 10(13): 1589–1602.

An P., Chen F., Li Z., Ling Y., Peng Y., Zhang H., Li J., Chen Z., and Wang H. 2020. HDAC8 Promotes the Dissemination of Breast Cancer Cells via AKT/GSK-3β/Snail Signals. *Oncogene*. 39(26): 4956–69.

Balasubramanian S., Ramos J., Luo W., Sirisawad M., Verner E., and Buggy J. J., 2008. A Novel Histone Deacetylase 8 (HDAC8)-Specific Inhibitor PCI-34051 Induces Apoptosis in T-Cell Lymphomas. *Leukemia*. 22(5): 1026–34.

Ben-Shahar T. R., Heeger S., Lehane C., East P., Flynn H., Skehel M., and Uhlmann F., 2008. Eco1-Dependent Cohesin Sister Chromatid Cohesion. *Science.* 321(5888): 563–66.

Bloom K., 2004. Microtubule Composition: Cryptography of Dynamic Polymers. *Proceedings of the National Academy of Sciences of the United States of America*. 101(18): 6839–40.

Brachmann W., 1916. Ein Fall von Symmetrischer Monodaktylie Durch Ulnadefekt, Mit Symmetrischer FLughautbildung in Den Ellenbeugen, Sowie Anderen Abnormitaten (Zwerghaftogkeit, Halsrippen, Behaarung). *Jarb Kinder Phys Erzie.* 84: 225–235.

Budillon A., Gennaro E. D., Bruzzese F., Rocco M., Manzo G., and Caraglia M., 2007. Histone Deacetylase Inhibitors: A New Wave of Molecular Targeted Anticancer Agents. *Recent Patents on Anti-Cancer Drug Discovery*. 2(2): 119–34.

Buggy J. J., Sideris M. L., Mak P., Lorimer D. D., Mcintosh B., and Clark J. M., 2000. Cloning and Characterization of a Novel Human Histone Deacetylase, HDAC8.

Biochemical Journal. 350(1): 199–205.

Busque L., Zhu J., DeHart D., Griffith B., Willman C., Carroll R., Black M. P., and Gilliland D. G., 1994. An Expression Based Clonality Assay at the Human Androgen Receptor Locus (HUMARA) on Chromosome X. *Nucleic Acids Research.* 22(4): 697–98.

Chakrabarti A., Oehme I., Witt O., Oliveira G., Sippl W., Romier C., Pierce R. J., and Jung M., 2015. HDAC8: A Multifaceted Target for Therapeutic Interventions. *Trends in Pharmacological Sciences.* 36(7): 481–92.

Chyra Z., Gkotzamanidou M., Shammas M. A., Souliotis V. L., Xu Y., Samur M. K., Beeler A. B. Hajek R., Fulciniti M., and Munshi N. C., 2019. HDAC8 Maintain Cytoskeleton Integrity Via Homologous Recombination and Represent a Novel Therapeutic Target in Multiple Myeloma. *Blood.* 134: 4385–4385.

ClinVar. Available at: https://www.ncbi.nlm.nih.gov/clinvar/ (Accessed: October 5th, 2020).

Cooper G. M., and Hausman R. E., 2000.The Cell. *Sinauer Associates Sunderland*. Chapter 4. The Organization of Cellular Genomes.

Dasgupta T., Antony J., Braithwaite H. W., and Horsfield J. A., 2016. HDAC8 Inhibition Blocks SMC3 Deacetylation and Delays Cell Cycle Progression without Affecting Cohesin-dependent Transcription in MCF7 Cancer Cells. *Journal of Biological Chemistry*. 291(24): 12761-770.

dbSNP. Available at: https://www.ncbi.nlm.nih.gov/snp/ (Accessed: October 5th, 2020).

De Ruijter A. J. M., Gennip A.H.V., Caron H.N., Kemp S., and Kuilenburg A.B.P.V., 2003. Histone Deacetylases (HDACs): Characterization of the Classical HDAC Family. *Biochemical Journal.* 370(3): 737–49.

Deardorff M. A., Bando M., et al., 2012. HDAC8 Mutations in Cornelia de Lange Syndrome Affect the Cohesin Acetylation Cycle. *Nature.* 489(7415): 313–17.

Deardorff M. A., Kaur. M., et al., 2007. Mutations in Cohesin Complex Members SMC3 and SMC1A Cause a Mild Variant of Cornelia de Lange Syndrome with Predominant Mental Retardation. *American Journal of Human Genetics.* 80(3): 485–94.

Deardorff M. A., Porter N. J., and Christianson D. W., 2016. Structural Aspects of HDAC8 Mechanism and Dysfunction in Cornelia de Lange Syndrome Spectrum Disorders. *Protein Science*: 25(11): 1965–76.

Deardorff M. A., Wilde J. J., et al., 2012. RAD21 Mutations Cause a Human Cohesinopathy. *American Journal of Human Genetics.* 90(6): 1014–27.

deLangeC., 1933. Suruntypenouveaudedegenerescence(Typus Amstelodamensis).

Arch Med Enfants. 36: 713–719.

Dokmanovic M., Clarke C., and Marks P. A., 2007. Histone Deacetylase Inhibitors: Overview and Perspectives. *Molecular Cancer Research.* 5(10): 981–89.

Dose A., Liokatis S., Theillet F. X., Selenko P., and Schwarzer D., 2011. NMR Profiling of Histone Deacetylase and Acetyl-Transferase Activities in Real Time. *ACS Chemical Biology.* 6(5): 419–24.

Durst K. L., Lutterbach B., Kummalue T., Friedman A. D., and Hiebert S. W., 2003. The Inv(16) Fusion Protein Associates with Corepressors via a Smooth Muscle Myosin Heavy-Chain Domain. *Molecular and Cellular Biology.* 23(2): 607–19.

Emmons M. F., Faião-Flores F. et al., 2019. HDAC8 Regulates a Stress Response Pathway in Melanoma to Mediate Escape from BRAF Inhibitor Therapy. *Cancer Research*. 79(11): 2947–61.

Ensembl. Available at: https://www.ensembl.org/index.html (Accessed: September 9th, 2020).

Fang H., Disteche C. M, and Berletch J. B., 2019. X Inactivation and Escape: Epigenetic and Structural Features. *Frontiers in Cell and Developmental Biology*. 7: 219.

Gallinari P., Marco S. D., Jones P., Pallaoro M., and Steinkühler C., 2007. HDACs, Histone Deacetylation and Gene Transcription: From Molecular Biology to Cancer Therapeutics. *Cell Research.* 17(3): 195–211.

Gao J., Siddoway B., Huang Q., and Xia H., 2009. Inactivation of CREB Mediated Gene Transcription by HDAC8 Bound Protein Phosphatase. *Biochemical and Biophysical Research Communications.* 379(1): 1–5.

Gao S., Chen C., Wang L., Hong L., Wu J., Dong P., and Yu F., 2013. Histone Deacetylases Inhibitor Sodium Butyrate Inhibits JAK2/STAT Signaling through Upregulation of SOCS1 and SOCS3 Mediated by HDAC8 Inhibition in Myeloproliferative Neoplasms. *Experimental Hematology.* 41(3): 261-270.

Glotzer M., 2001. Animal Cell Cytokinesis. *Molecular Pathology.* 17: 351–86.

Gregoretti I. V., Lee Y., and Goodson H. V., 2004. Molecular Evolution of the Histone Deacetylase Family: Functional Implications of Phylogenetic Analysis. *Journal of Molecular Biology.* 338(1): 17–31.

Haberland M., Montgomery R. L., and Olson E. N., 2009. The many roles of histone deacetylases in development and physiology: implications for disease and therapy. Nature Reviews Genetics. 10(1): 32–42.

Han L., Ge J., Zhang L., Ma R., Hou X., Li B., Moley K., and Wang Q., 2015. Sirt6 Depletion Causes Spindle Defects and Chromosome Misalignment during Meiosis of Mouse Oocyte. *Scientific Reports.* 5: 1–10.

Harakalova M. Boogaard M. V. D., et al., 2012. X-Exome Sequencing Identifies a HDAC8 Variant in a Large Pedigree with X-Linked Intellectual Disability, Truncal Obesity, Gynaecomastia, Hypogonadism and Unusual Face. *Journal of Medical Genetics.* 49(8): 539–43.

Heidinger-Pauli J. M., Ünal E., and Koshland D., 2009. Distinct Targets of the Eco1 Acetyltransferase Modulate Cohesion in S Phase and in Response to DNA Damage. *Molecular Cell.* 34(3): 311–21.

Higuchi T., Nakayama T., Arao T., Nishio K., and Yoshie O., 2013. SOX4 Is a Direct Target Gene of FRA-2 and Induces Expression of HDAC8 in Adult T-Cell Leukemia/Lymphoma. *Blood.* 121(18): 3640–49.

Hu E., Chen Z., Fredrickson T., Zhu Y., Kirkpatrick R., Zhang G., Johanson K., Sung C., Liu R., and Winkler J., 2000. Cloning and Characterization of a Novel Human Class I Histone Deacetylase That Functions as a Transcription Repressor. *Journal of Biological Chemistry.* 275(20): 15254–64.

Ishii S., Kurasawa Y., Wong J., and Yu-Lee L., 2008. Histone deacetylase 3 localizes to the mitotic spindle and is required for kinetochore-microtubule attachment. *Proceedings of the National Academy of Sciences of the United States of America*. 105(11): 4179-4184.

Jamaladdin S., Kelly R. D. W., et al., 2014. Histone deacetylase (HDAC) 1 and 2 are essential for accurate cell division and the pluripotency of embryonic stem cells. *Proceedings of the National Academy of Sciences of the United States of America*. 111(27): 9840-9845.

Kaiser F. J., Ansari M. et al., 2014. Loss-of-Function HDAC8 Mutations Cause a Phenotypic Spectrum of Cornelia de Lange Syndrome-like Features, Ocular Hypertelorism, Large Fontanelle and X-Linked Inheritance. *Human Molecular Genetics.* 23(11): 2888–2900.

Kang Y., Nian H., et al., 2014. HDAC8 and STAT3 Repress BMF Gene Activity in Colon Cancer Cells. *Cell Death and Disease.* 5(10): 1–8.

Kapoor T.M., Lampson M.A., Hergert P., Cameron L, Cimini D., Salmon E.D., McEwen B.F., and Khodjakov A., 2006. Chromosomes Can Congress to the Metaphase Plate before Biorientation. *Science.* 311: 388–91.

Karolczak-Bayatti M., Sweeney M., Cheng J., Edey L., Robson S. C., Ulrich S. M., Treumann A., Taggart M. J., and Europe-Finner G. N., 2011. Acetylation of Heat Shock Protein 20 (Hsp20) Regulates Human Myometrial Activity. *Journal of Biological Chemistry.* 286(39): 34346–55.

Killick R., Niklison-Chirou M. et al., 2011. P73: A Multifunctional Protein in Neurobiology.

Molecular Neurobiology. 43(2): 139–46.

Kline A. D., Moss J. F. et al., 2018. Diagnosis and Management of Cornelia de Lange Syndrome: First International Consensus Statement. *Nature Reviews Genetics.* 19(10): 649–66.

Kollman J. M., Merdes A., Mourey L., and Agard D. A., 2011. Microtubule Nucleation by γ-Tubulin Complexes. *Nature Reviews Molecular Cell Biology.* 12(11): 709–21.

Krantz I. D., McCallum J. et al., 2004. Cornelia de Lange Syndrome Is Caused by Mutations in NIPBL, the Human Homolog of Drosophila Melanogaster Nipped-B. *Nature Genetics*. 36(6): 631–35.

Kutil Z., Novakova Z., Meleshin M., Mikesova J., Schutkowski M., and Barinka C., 2018. Histone Deacetylase 11 Is a Fatty-Acid Deacylase. *ACS Chemical Biology.* 13(3): 685–93.

Lampson M. A., and Grishchuk E. L., 2017. Mechanisms to Avoid and Correct Erroneous Kinetochore-Microtubule Attachments. *Biology.* 6(1).

Lee H., Rezai-Zadeh N., and Seto E., 2004. Negative Regulation of Histone Deacetylase 8 Activity by Cyclic AMP-Dependent Protein Kinase A. *Molecular and Cellular Biology.* 24(2): 765–73.

Lee H., Sengupta N.,Villagra A., Rezai-Zadeh N., and Seto E., 2006. Histone Deacetylase 8 Safeguards the Human Ever-Shorter Telomeres 1B (HEST1B) Protein from Ubiquitin-Mediated Degradation. *Molecular and Cellular Biology.* 26(14): 5259–69.

Li J., Chen S., Cleary R. A., Wang R., Gannon O. J., Seto E., and Tang D.D., 2014. Histone Deacetylase 8 Regulates Cortactin Deacetylation and Contraction in Smooth Muscle Tissues. *American Journal of Physiology - Cell Physiology*. 307: C288–C295.

Liu J., and Krantz I. D., 2009. Cornelia de Lange Syndrome, Cohesin, and Beyond. *Clinical Genetics.* 76(4): 303–14.

Liu P.,Tarle S. A.,Hajra A., Claxton D. F., Marlton P., Freedman M., Siciliano M. J., and Collins F. S., 1993. Fusion between Transcription Factor CBF Beta/PEBP2 Beta and a Myosin Heavy Chain in Actue Myeloid Leukemia. *Science.* 261(5124): 1041–44.

Lopez G., Bill K.L. J., Bid H. K., Braggio D., Constantino D., Prudner B., Zewdu A., Batte K., Lev D., and Pollock R. K., 2015. HDAC8, A Potential Therapeutic Target for the Treatment of Malignant Peripheral Nerve Sheath Tumors (MPNST). *PLoS ONE.* 10(7): 1–12.

Mannini L., Cucco F., Quarantotti V., Krantz I. D., and Musio A., 2013. Mutation Spectrum and Genotype-Phenotype Correlation in Cornelia de Lange Syndrome. *Human Mutation.* 34(12): 1589–96.

Marek M., Kannan S. et al., 2013. Structural Basis for the Inhibition of Histone Deacetylase 8 (HDAC8), a Key Epigenetic Player in the Blood Fluke Schistosoma Mansoni. *PLoS Pathogens.* 9(9): e1003645

Meunier S., and Vernos I., 2012. Microtubule Assembly during Mitosis - from Distinct Origins to Distinct Functions? *Journal of Cell Science.* 125(12): 2805–14.

Mitelman F., and Heim S., 1992. Quantitative Acute Leukemia Cytogenetics. *Genes, Chromosomes and Cancer.* 5(1): 57–66.

Muraoka R.S., Dumont N., et al., 2002. Blockade of TGF- β Inhibits Mammary Tumor Cell Viability, Migration, and Metastases. *J.Clin.Invest.* 109(12): 1551–59.

Nasmyth K., and Haering C.H., 2009. Cohesin: Its Roles and Mechanisms. *Annual Review of Genetics.* 43(1): 525–58.

NCBI. Available at: https://www.ncbi.nlm.nih.gov/gene/?term=. (Accessed: September 10th, 2020)

Nian H., Bisson W.H., Dashwood W., Pinto J.T., and Dashwood R.H., 2009. α-Keto Acid Metabolites of Organoselenium Compounds Inhibit Histone Deacetylase Activity in Human Colon Cancer Cells. *Carcinogenesis.* 30(8): 1416–23.

O'Connor C. 2008. Cell Division: Stages of Mitosis. *Nature Education*. 1:188.

Oehme I., Deubzer H. E., et al., 2009. Histone Deacetylase 8 in Neuroblastoma Tumorigenesis. *Clinical Cancer Research.* 15(1): 91–99.

OMIM. Available at: https://www.omim.org/ (Accessed:October 15th, 2020).

Oslon D. E., Udeshi N. D. et al., 2014. An Unbiased Approach to Identify Endogenous Substrates of 'Histone' Deacetylase 8. *ACS Chemical Biology.* 9(10): 2210–16.

Park S., Yoo H., Seol J. H., and Rhee K., 2019. HDAC3 and HDAC8 Are Required for Cilia Assembly and Elongation. *Biology Open.* 8(8): bio043828.

Park S. Y., Jun I. A., Jeong K. J., Heo H. J., Sohn J. S., Lee H. Y., Park C. H., and Kang J., 2011. Histone Deacetylases 1, 6 and 8 Are Critical for Invasion in Breast Cancer. *Oncology Reports.* 25(6): 1677–81.

Paweletz N., 2001. Walther Flemming : Pioneer of Mitosis Research. 2(1): 72–75.

Porter N. J., Christianson N. H., Decroos C., and Christianson D. W., 2016. Structural and Functional Influence of the Glycine-Rich Loop G302GGGY on the Catalytic Tyrosine of Histone Deacetylase 8. *Biochemestry*. 55(48): 6718–6729.

Qi J., Singh S., et al., 2015. HDAC8 Inhibition Specifically Targets Inv(16) Acute Myeloid Leukemic Stem Cells by Restoring p53 Acetylation. *Cell Stem Cell*. 17(5): 597-610.

Qian Y., Zhang J., Jung Y., and Chen X., 2014. DEC1 Coordinates with HDAC8 to Differentially Regulate TAp73 and ΔNp73 Expression. *PLoS ONE.* 9(1): e84015.

Ramos F. J., Puisac B., et al., 2015. Clinical Utility Gene Card for: Cornelia de Lange Syndrome. *European Journal of Human Genetics.* 23(10): 1–4.

Ried T., Hu Y., Difilippantonio M.J., Ghadimi B.M., Grade M., and Camps J., 2012. The Consequences of Chromosomal Aneuploidy on the Transcriptome of Cancer Cells. *Biochimica et Biophysica Acta - Gene Regulatory Mechanisms.* 1819(7): 784–93.

Rieder C. L., 1982. The Formation, Structure, and Composition of the Mammalian Kinetochore and Kinetochore Fiber. *International Review of Cytology.* 79:1-58.

Rieder C.L., and Salmon E., 1998. The Vertebrate Cell Kinetochore and Its Roles during Mitosis. *Trends in Cell Biology* 8: 310–18.

Santos-Barriopedro I., Li Y., Bahl S., and Seto E., 2019. Hdac8 Affects Mgmt Levels in Glioblastoma Cell Lines via Interaction with the Proteasome Receptor Adrm1. *Genes and Cancer.* 10(5–6): 119–33.

Schnerch D., and Nigg E. A., 2016. Structural Centrosome Aberrations Favor Proliferation by Abrogating Microtubule-Dependent Tissue Integrity of Breast Epithelial Mammospheres. *Oncogene.* 35(21): 2711–22.

Sen S., 2000. Aneuploidy and Cancer. *Current Opinion in Oncology.* 12(1): 82–88.

Seto E., and Yoshida M., 2014. Erasers of Histone Acetylation: The Histone Deacetylase Enzymes. *Cold Spring Harbor Perspectives in Biology.* 6(4): a018713.

Singh V. P., Yueh W., Gerton J. L., and Duncan F. E., 2019. Oocyte-Specific Deletion of Hdac8 in Mice Reveals Stage-Specific Effects on Fertility. *Reproduction.* 157(3): 305–16.

Song S., Wang Y., XU P., Yang R., Ma Z., Liang S., and Zhang G., 2015. The Inhibition of Histone Deacetylase 8 Suppresses Proliferation and Inhibits Apoptosis in Gastric Adenocarcinoma. *International Journal of Oncology* 47(5): 1819–28.

Banerjee S., Adhikari N., Amin Sk A., and Jha T., 2019. Histone Deacetylase 8 (HDAC8) and Its Inhibitors with Selectivity to Other Isoforms: An Overview. *European Journal of Medicinal Chemistry.* 164: 214–40.

Tang X., Li G., et al., 2020. HDAC8 Cooperates with SMAD3/4 Complex to Suppress SIRT7 and Promote Cell Survival and Migration. *Nucleic Acids Research.* 48(6): 2912–2923.

Taunton J., Hassig C. A., and Schreiber S. L., 1996. A Mammalian Histone Deacetylase Related to the Yeast Transcriptional Regulator Rpd3p. *Science.* 272(5260): 408–11.

The Human Protein Atlas. Available at: https://www.proteinatlas.org/ (Accessed:

September 20th, 2020).

Tonkin E.T., Wang T., Lisgo S., Bamshad M.J., Strachan T., 2004. NIPBL, Encoding a Homolog of Fungal Scc2-Type Sister Chromatid Cohesion Proteins and Fly Nipped-B, Is Mutated in Cornelia de Lange Syndrome. *Nature Genetics.* 36(6): 636–41.

Uhlmann F., Lottspelch F., and Nasmyth K., 1999. Sister-Chromatid Separation at Anaphase Onset Is Promoted by Cleavage of the Cohesin Subunit Scc1. *Nature.* 400(6739): 37–42.

Ünal E., Heidinger-Pauli J. M., Kim W., Guacci V., Onn I., Gygi S. P., and Koshland D. E., 2008. A Molecular Determinant for the Establishment of Sister Chromatid Cohesion. *Science.* 321(5888): 566–69.

UniProt. Available at: https://www.uniprot.org/ (Accessed: September 20th, 2020).

Wyngaert I. V. D, Vries W. D., Kremer A., Neefs J., Walter H. M. L., and Kass A. U., 2000. Cloning and Characterization of Human Histone Deacetylase 8. *FEBS Letters* 478(1–2): 77–83.

Vanaja G.R., Ramulu H.G., and Kalle A.M., 2018. Overexpressed HDAC8 in Cervical Cancer Cells Shows Functional Redundancy of Tubulin Deacetylation with HDAC6. *Cell Communication and Signaling.* 16(1): 1–16.

Vannini A., Volpari C., et al., 2004. Crystal Structure of a Eukaryotic Zinc-Dependent Histone Deacetylase, Human HDAC8, Complexed with a Hydroxamic Acid Inhibitor. *Proceedings of the National Academy of Sciences of the United States of America.* 101(42): 15064–69.

Verma L., Passi S., and Gauba K., 2010. Brachman de Lange syndrome. *Contemporary Clinical Dentistry.* 1(4): 268–270.

Ververis K., Hiong A., Karagiannis T. C., and Licciardi P. V., 2013. Histone Deacetylase Inhibitors (HDACIS): Multitargeted Anticancer Agents. *Biologics: Targets and Therapy.* 7(1): 47–60.

Wang P., Zhang Y., Wang B., Liu J., Wang Y., Pan D., Wu X., Fang W. K., and Zhou J., 2019. A Statistical Measure for the Skewness of X Chromosome Inactivation Based on Case-Control Design. *BMC Bioinformatics.* 20(1): 1–14.

Waltregny D., Leval L. D., Glénisson W., Tran S. L., North B. J., Bellahcène A., Weidle U., Verdin E., and Castronovo V., 2004. Expression of Histone Deacetylase 8, a Class I Histone Deacetylase, Is Restricted to Cells Showing Smooth Muscle Differentiation in Normal Human Tissues. *American Journal of Pathology.* 165(2): 553–64.

Waltregny D., Glénisson W., Tran S. L., North B. J., Verdin E., Colige A., and Castronovo

V., 2005. Histone Deacetylase HDAC8 Associates with Smooth Muscle α-actin and Is Essential for Smooth Muscle Cell Contractility. *The FASEB Journal.* 19(8): 966–68.

Watrin E., and Peters J., 2009. The Cohesin Complex Is Required for the DNA Damage-Induced G2/M Checkpoint in Mammalian Cells. *EMBO Journal.* 28(17): 2625–35.

Wilson B. J., Tremblay A. M., Deblois G., Sylvain-Drolet G., and Giguère V., 2010. An Acetylation Switch Modulates the Transcriptional Activity of Estrogen-Related Receptor α. *Molecular Endocrinology.* 24(7): 1349–58.

Witt O., Deubzer H.E., Milde T., and Oehme I., 2009. HDAC Family: What Are the Cancer Relevant Targets? *Cancer Letters.* 277(1): 8–21.

Wolfson N. A., Pitcairn C. A., and Fierke C. A., 2013. HDAC8 Substrates: Histones and Beyond. *Biopolymers.* 99(2): 112–26.

Wu J., Du C., Lv Z., Ding C., Cheng J., Xie H., Zhou L., and Zheng S., 2013. The Up-Regulation of Histone Deacetylase 8 Promotes Proliferation and Inhibits Apoptosis in Hepatocellular Carcinoma. *Digestive Diseases and Sciences.* 58(12): 3545–53.

Yamauchi Y., Boukari H., Banerjee I., Sbalzarini I. F., Horvath P. Helenius A., 2011. Histone Deacetylase 8 Is Required for Centrosome Cohesion and Influenza a Virus Entry. *PLoS Pathogens* 7(10): e1002316.

Yan W., Liu S., Xu E., Zhang J., Zhang Y., Chen X., and Chen X., 2013. Histone Deacetylase Inhibitors Suppress Mutant P53 Transcription via Histone Deacetylase 8.*Oncogene.* 32(5): 599–609.

Yang W., Tsai S., Wen Y., Fejér G., and Seto E., 2002. Functional Domains of Histone Deacetylase-3. *Journal of Biological Chemistry.* 277(11): 9447–54.

Yuan B., Neira J. et al., 2019. Clinical Exome Sequencing Reveals Locus Heterogeneity and Phenotypic Variability of Cohesinopathies. *Genetics in Medicine.* 21(3): 663–75.

Zhang K., Lu Y., Jiang C., Liu W., Shu J., Chen X., Shi Y., Wang E., Wang L., Hu Q., Dai Y., and Xiong B., 2017. HDAC8 Functions in Spindle Assembly during Mouse Oocyte. *Oncotarget.* 8(12): 20092-20102

Zhang Y., Li N., Caron C., Matthias G., Hess D., Khochbin S., and Matthias P. 2003. HDAC-6 interacts with and deacetylates tubulin and microtubules in vivo. *EMBO Journal.* 22(5): 1168-1179.